

TLR4 exhibits a Pivotal Role in Immuno-Oncology through Systematic Pan-Cancer Analysis

Yuan Wang¹, Lehui Du¹, Yanan Han¹, Pei Zhang¹, Xiang Huang¹, Qian Zhang¹, Yan Wang¹, Xingdong Guo¹, Xin Tan², Jiangyue Lu², Qingchao Shang², Yawei Bi³, Xiao Lei¹, and Baolin Qu¹

¹Chinese PLA General Hospital

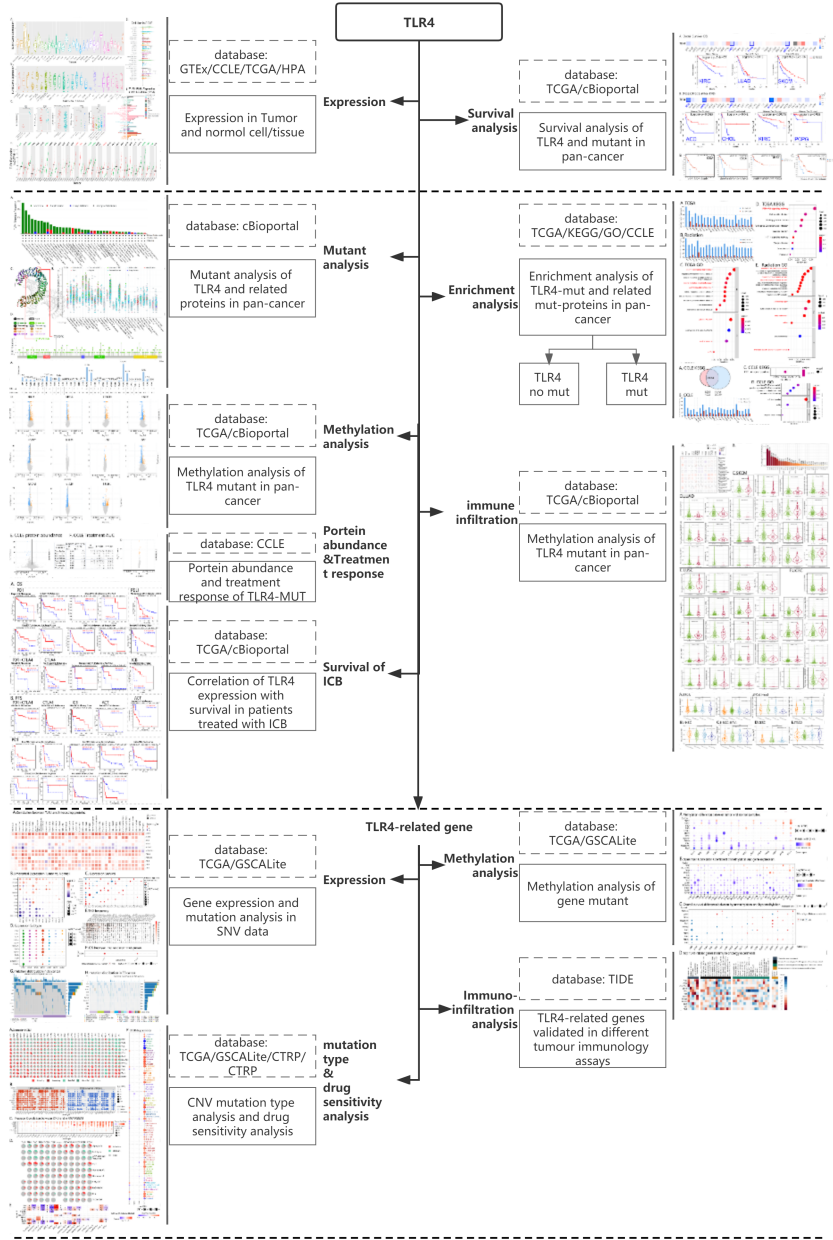
²Medical School of Chinese PLA

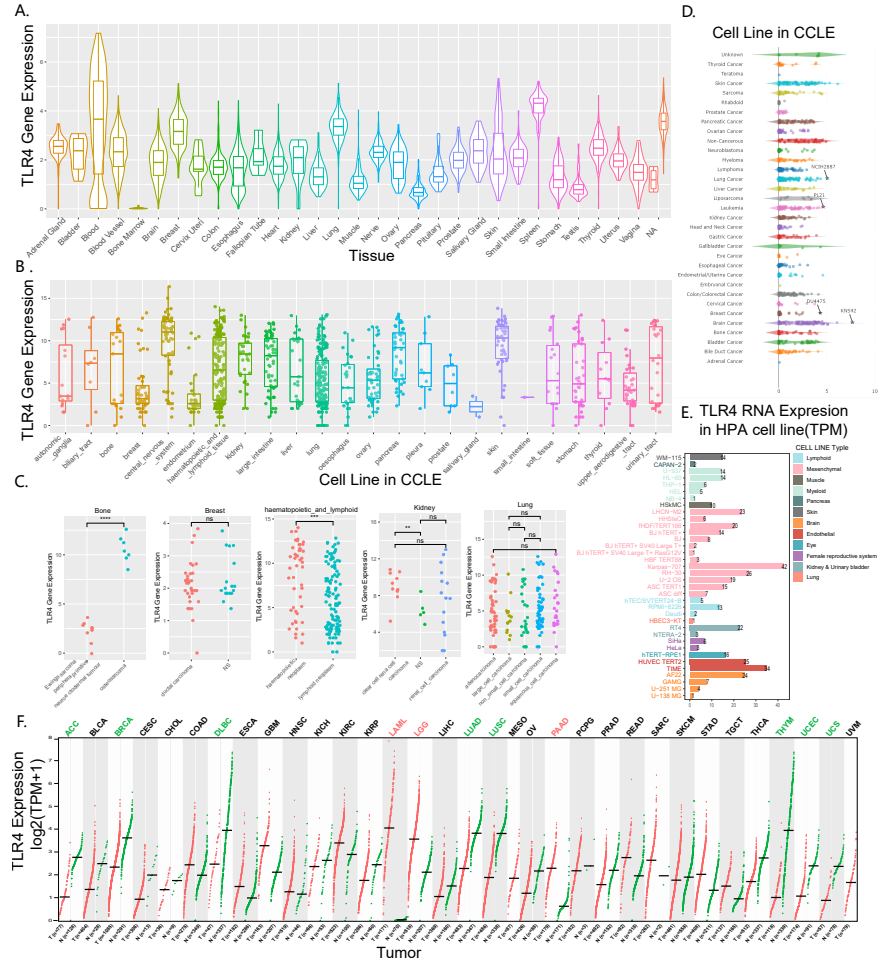
³The First Medical Center of PLA General Hospital

March 23, 2023

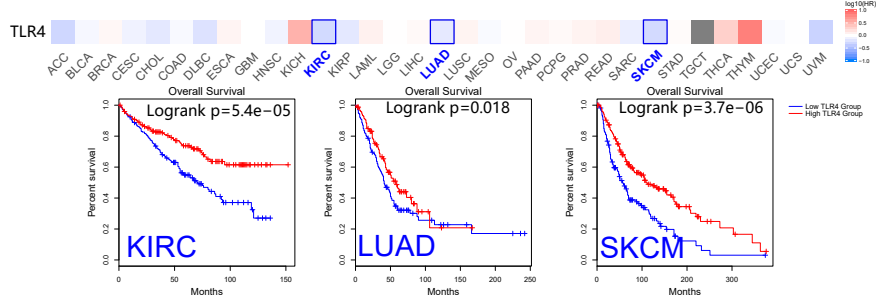
Abstract

The role of TLR4 (toll like receptor 4), a key molecule of the classical innate immune pathway, in individual tumors requires further exploration. In this study, numerous databases and tools, such as TCGA, GTEx, cBioportal, GSCALite, and GDSC, were utilized to systematically analyze the prognostic and immunological potential of TLR4 in tumors. The expression levels and mutational dynamics of TLR4 in pan-cancer were investigated. The prognostic potential of TLR4 was analyzed using Kaplan-Meier (KM) analysis. Results showed the levels of TLR4 in tumor tissues were significantly lower as compared to those in normal tissues in most cancers and were strongly correlated with the patient's outcomes. The mutant genes associated with TLR4 were mainly enriched in the PI3K-AKT pathway. This could be a potential pathway for radiotherapy to activate the tumor immune microenvironment via TLR4/MAP. In tumors, the TLR4 mutations were closely associated with the M1/M2 polarization of macrophages. TLR4 and its ligand CD14 were significantly negatively associated with immunosuppressed MDSCs and TAM M2. The intervention of TLR4-dependent signaling pathways might be a promising strategy to reduce tolerance to ICB treatment in the post-immune era. In conclusion, this study expands the potential of TLR4 as an immune target in tumor therapy.

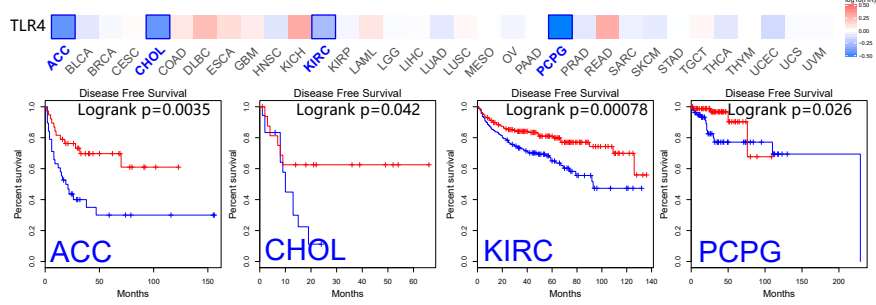


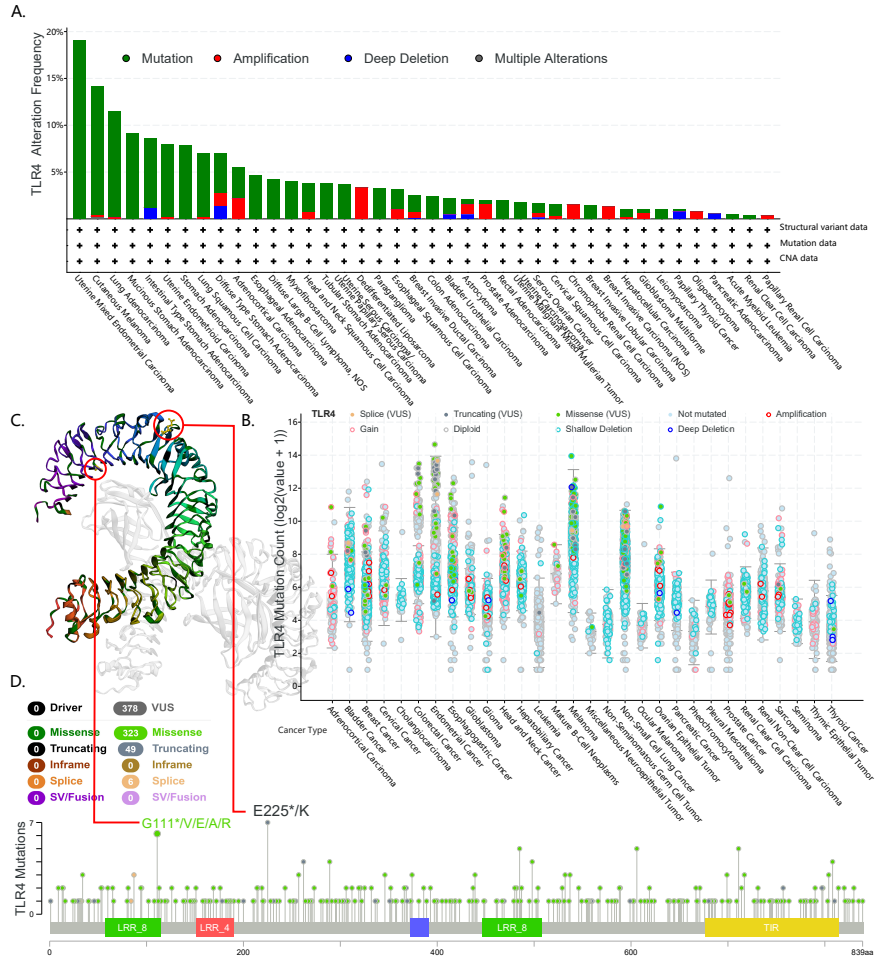


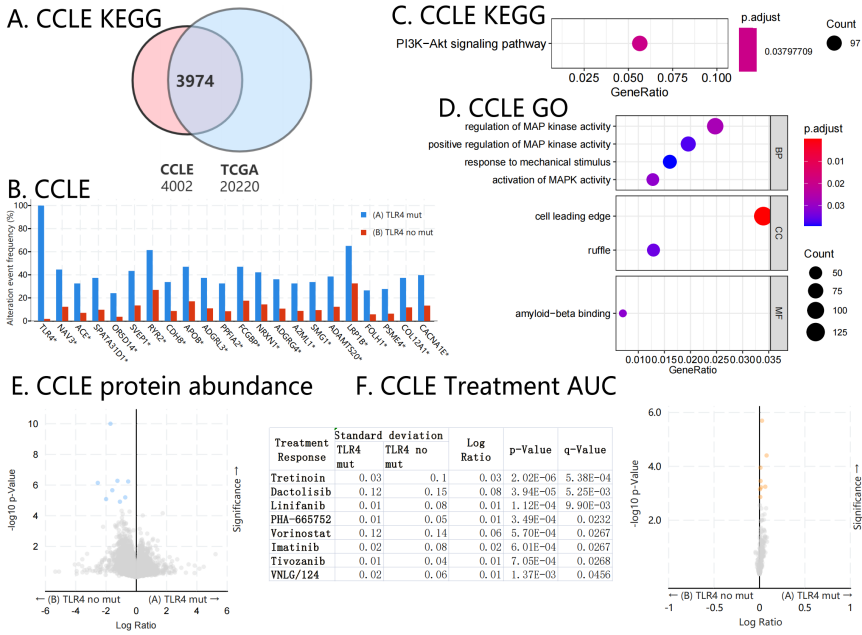
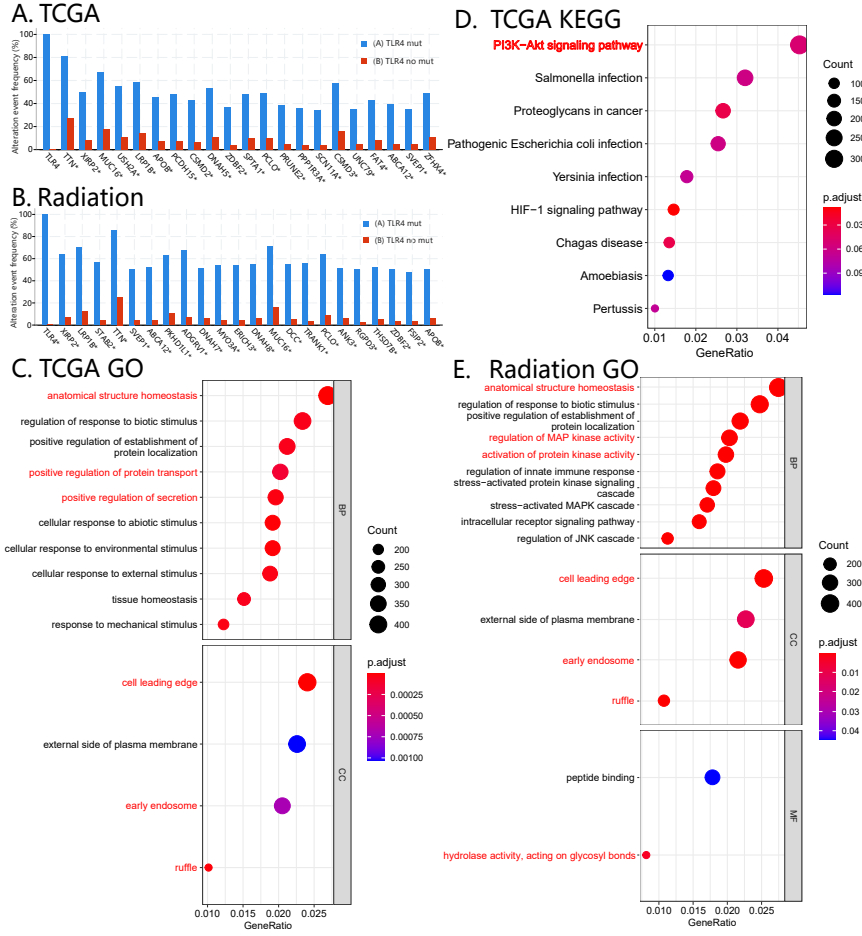
A. Overall Survival (OS)

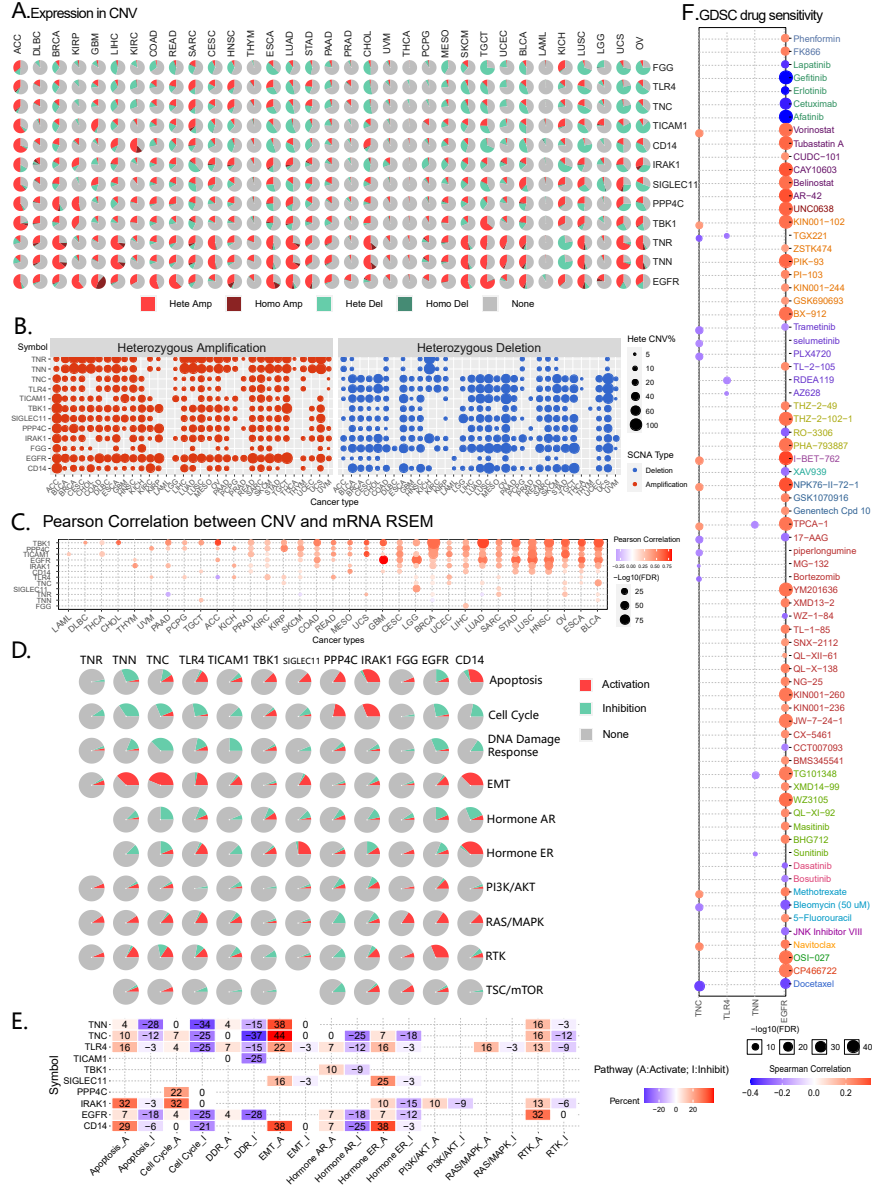


B. Disease Free Survival (DFS)









Title page

***TLR4* exhibits a Pivotal Role in Immuno-Oncology through Systematic Pan-Cancer Analysis**

Yuan Wang 1#, Lehui Du 1#, Yanan Han 1#, Pei Zhang 1, Xiang Huang 1, Qian Zhang 1, Yan Wang 1, Xingdong Guo 1,2, Xin Tan 1,2, Jiangyue Lu 1,2, Qingchao Shang 1,2, Yawei Bi 3*, Xiao Lei 1*, Baolin Qu 1*

1. Department of Radiation Oncology, Chinese PLA General Hospital, Beijing, China.

2. Medical School of Chinese PLA, Beijing, China.

3. Department of Gastroenterology and Hepatology, The First Medical Center of PLA General Hospital, Beijing, China

*Corresponding author: Baolin Qu, Xiao Lei, Yawei Bi

#Contributed equally: Yuan Wang, Lehui Du, Yanan Han

Address: Department of Radiation Oncology, The First Medical Center of PLA General Hospital, Beijing, China.

E-mail: baolinqu301@163.com, leixiao@301hospital.com.cn, 530713082@qq.com

Keywords: Toll like receptor 4, Pan cancer analysis, immunotherapy

Abstract

The role of *TLR4* (toll like receptor 4), a key molecule of the classical innate immune pathway, in individual tumors requires further exploration. In this study, numerous databases and tools, such as TCGA, GTEx, cBioportal, GSCALite, and GDSC, were utilized to systematically analyze the prognostic and immunological potential of *TLR4* in tumors. The expression levels and mutational dynamics of *TLR4* in pan-cancer were investigated. The prognostic potential of *TLR4* was analyzed using Kaplan-Meier (KM) analysis. Results showed the levels of *TLR4* in tumor tissues were significantly lower as compared to those in normal tissues in most cancers and were strongly correlated with the patient's outcomes. The mutant genes associated with *TLR4* were mainly enriched in the PI3K-AKT pathway. This could be a potential pathway for radiotherapy to activate the tumor immune microenvironment via *TLR4*/MAP. In tumors, the *TLR4* mutations were closely associated with the M1/M2 polarization of macrophages. *TLR4* and its ligand CD14 were significantly negatively associated with immunosuppressed MDSCs and TAM M2. The

intervention of *TLR4*-dependent signaling pathways might be a promising strategy to reduce tolerance to ICB treatment in the post-immune era. In conclusion, this study expands the potential of TLR4 as an immune target in tumor therapy.

Introduction

Cancer has become one of the major barriers to increasing life expectancy and is globally ranked as a leading cause of death worldwide. In the United States, 1,918,030 new cancer cases and 609,360 deaths were expected to occur due to cancer in 2022 ^[1]. It is projected that 30 million new cancer cases and nearly 17 million cancer-related deaths will occur each year by 2040 ^[2].

Tumor cells are not destroyed by the immune system and can cause inflammation in tumor tissues. Tumor microenvironment (TME) is defined as heterogeneous and interacting populations of cancer cells, cancer stem cells, and multiple recruited stromal cell types, such as transformed parenchyma and associated stroma cells; TME and is now widely recognized to have an integral role in tumorigenesis and malignant progression ^[3]. The immune profiles of each tumor type are different, and the classification of this profile is becoming clearer and deeper ^[4]. Currently, the tumor is treated using a personalized immunotherapy strategy based on an immune profile. *TLR4* (toll like receptor 4) gene expresses in all cells in TME. It plays an important role in the innate and adaptive immune systems and inhibits the proliferation of tumors. A specific mechanism has recently been identified in some highly malignant and immunosuppressive tumors; these rapidly expanding tumors release signals called damage-associated molecular patterns (DAMPs). DAMPs subsequently activate TLRs, which have pro-inflammatory and anti-tumor effects in tumorigenesis. However, the malignant tumor cells can suppress *TLR4* expression to evade immunity ^[5]. Inhibiting the tumor progression through the agonism of *TLR4* or its upstream pathways has also been investigated; studies have shown that *TLR4* is an immune adjuvant, which promotes the efficiency of immunotherapy ^[6,7]. *TLR4* is known to be involved in radiation pneumonia, which is one of the most important side effects of radiotherapy. However, the exact mechanism has not been clearly studied to understand the role of *TLR4* as a double-edged sword in this field. A previous study reported that activating *TLR4* on the surface of macrophages promoted their polarization towards M1 and induced them to secrete exosomes, which provided protection against the damage caused by radiation ^[8]. There are differences in the expression and mutation status of *TLR4* in the progression, prognosis, and immunotherapy response in different tumor

types. Therefore, a deeper systematic analysis of pan-cancer is needed.

Materials and Methods

Pre-processing and collection of datasets

In the current study, the RNA-seq, single nucleotide variation (SNV), deletion/amplification of hetero/homozygous copy number variations (CNVs), and methylation data of 33 tumors were obtained from The Cancer Genome Atlas (TCGA) database (portal.gdc.cancer.gov). The samples with complete information on OS (overall survival) and DFS (disease free survival) were included. The MSS (data of solid tumor mutation) data and PFS data were used in the present study [9]. The data of normal tissue samples, which corresponded to the tumor types, were downloaded from the Genotype-Tissue Expression project (GTEx) dataset. The combined cohort of TCGA and GTEx samples were downloaded from Xena (xenabrowser.net/), and the batch effect was removed (CutAdapt was used for adapter trimming, STAR was used for alignment, and RSEM and Kallisto were used as quantifiers) [10]. Immunotherapy response-related data were collected from immunotherapeutic clinical trials using the TIDE (Tumor Immune Dysfunction and Exclusion) tool. The cell lines data were obtained from the Cancer Cell Line Encyclopedia (CCLE) [11] and Human Protein Atlas (HPA) [12] datasets.

Survival analysis

The correlation between *TLR4* expression/mutation and patient survival in different cancers was analyzed using Kaplan-Meier Plotter and CoxPH model.

Methylation and Mutation profile

The GSCALite platform (bioinfo.life.hust.edu.cn/web/GSCALite/) and cBioPortal (www.cbioportal.org) were used to analyze the differences in methylation of the *TLR4* gene between the tumor and normal tissues in various TCGA cancer types as well as the effects of *TLR4* expression and mutational differences on the methylation levels of tumor [13]. The SNV frequency, heterozygous/pure CNVs of *TLR4*-related genes, and correlations between CNVs and mRNA expression levels of these gene clusters were determined using GSCA.

Protein-protein interaction (PPI) analysis

The PPIs of *TLR4* proteins were analyzed using STRING (cn.string-db.org/) [14], and only the experimentally validated protein interaction data were included. The minimum required interaction score was set to 0.150.

Drug sensitivity analysis

The drug sensitivity analysis was performed using GDSC (www.cancerrxgene.org/)^[15] and CTRP (portals.broadinstitute.org/ctrp/)^[16] databases.

Analysis of immune cells infiltration in Tumor

Immune cell infiltration in tumor tissues was assessed using TIMER2.0 (timer.comp-genomics.org/)^[17]. Somatic copy number alterations (sCNAs) were identified using GISTIC 2.0, which estimated the sCNA information using the copy number segmentation profiles at the gene level, including “deep deletion”, “arm-level deletion”, “diploid/normal”, and “arm-level gain”^[18]. The function prediction of *TLR4*-related genes, which regulated tumor immune genes, and the immune dysfunction and rejection of tumor immune escape mechanism were analyzed using TIDE (tide.dfci.harvard.edu/)^[19]. These analyses were performed to effectively predict the effects of immune checkpoint suppression therapy and subsequent experimental plan.

Statistical analyses

The expression and mutation levels of *TLR4* in the tumor and corresponding normal tissues were compared using the Student’s *t*-test and the Kruskal-Wallis test. Log-rank test was used to explore the survival differences between *TLR4*-high and *TLR4*-low groups, based on OS and DFS. All tests were two-sided, and a *P*-value of <0.05 was considered statistically significant.

Results

The design flow chart of the current study is shown in Figure 1.

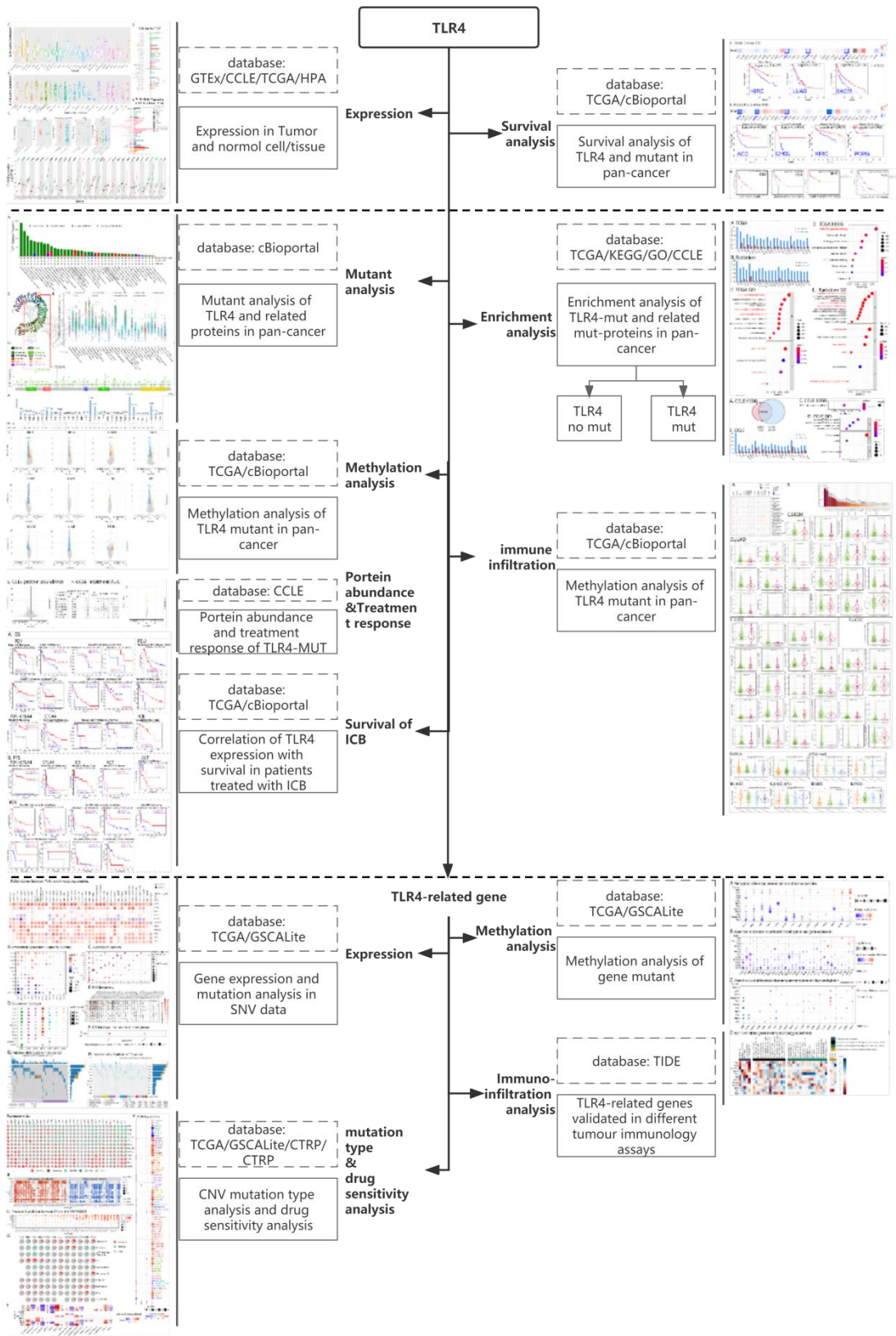


Figure 1 Design flow chart of the study.

1. Expression and prognostic potential of *TLR4*

1.1 Expression of *TLR4*

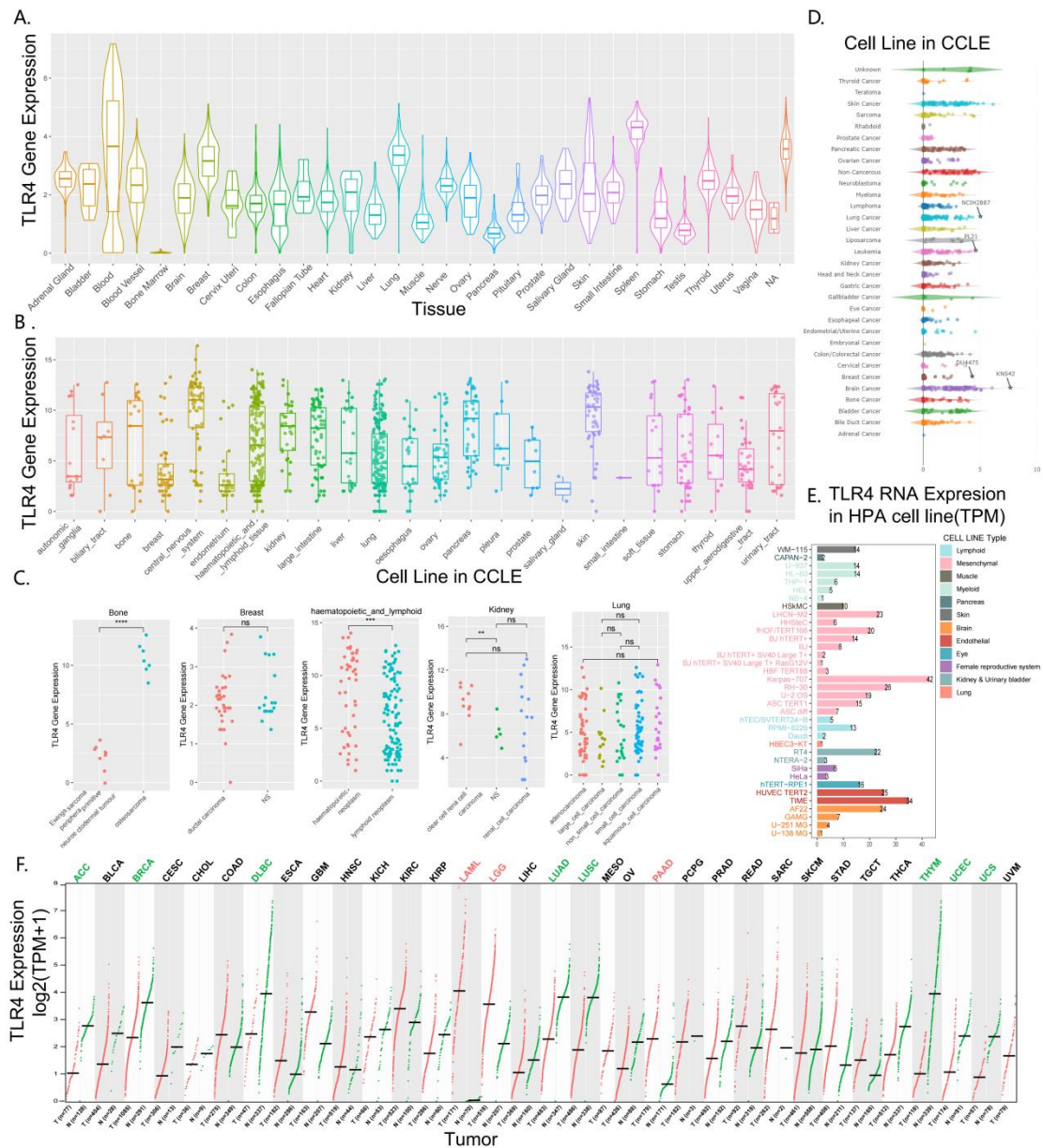
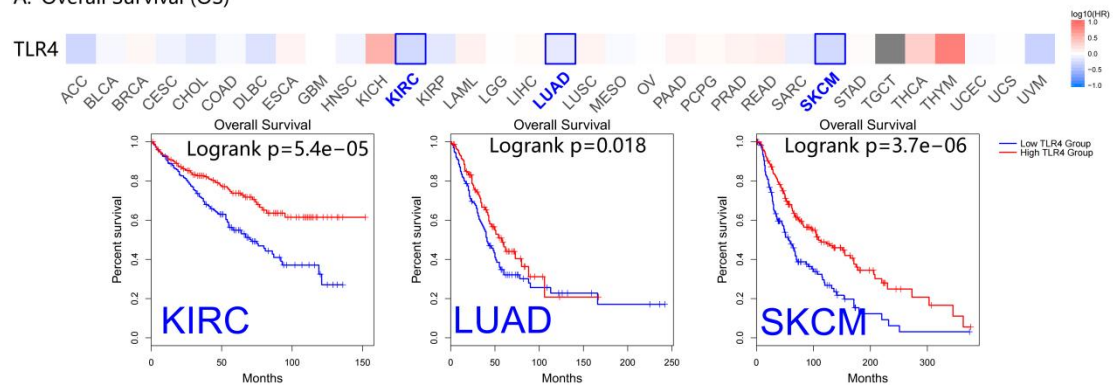


Figure 2 Expression landscape of *TLR4* in the normal and tumor samples. *TLR4* levels in 32 human tissues from the GETx dataset (A). *TLR4* levels in tumor cell lines from the CCL6 dataset (B-D). *TLR4* expression levels in 35 tumor cell lines from the HPA dataset (E). *TLR4* expression analyzed in tumor and normal tissue by TCGA and GETx datasets (F), using LIMMA methods, $|\log_2(\text{TPM} + 1)|$ Cutoff=1.2; q-value Cutoff=0.05.

The differences in the expression levels of *TLR4* were explored in normal and tumor tissues as well as tumor cells. Initially, the data on *TLR4* expression levels in 30 normal human tissues were obtained from the GTEx portal (Figure 2A). The top four *TLR4*-enriched tissues included spleen, blood, lung, and breast tissues. The CCL6 data showed that in tumor tissues, the highest

average expression of *TLR4* was found in the central nervous system, skin, and pancreas tissues (Figure 2B). The expression stratification of tumor cell lines in bone tissue was evident, showing that the expression level of *TLR4* in the osteosarcoma subgroup was significantly higher as compared to that in the Ewings sarcoma peripheral primitive neuron ectoderma tumor subgroup (Figure 2C). The highest *TLR4* expression was observed in NCIH2887 (lung cancer cell line), PL21(leukemia cell line), DU4475 (brain cancer cell line), and KNS42 (brain cancer cell line), as shown in Figure 2D. *TLR4* expression in the cell lines of each tumor in the HPA database was also analyzed (Figure 2E, Supplementary Table S1). The expression levels of genes in each cancer type were subsequently compared to those in the normal tissues. The results showed that ACC (Adrenocortical carcinoma), BRCA (Breast invasive carcinoma), DLBC (Lymphoid Neoplasm Diffuse Large B-cell Lymphoma), LUAD (Lung adenocarcinoma), LUSC (Lung squamous cell carcinoma), THYM (Thymoma), UCEC (Uterine Corpus Endometrial Carcinoma), and UCS (Uterine Carcinosarcoma) tumor tissues had significantly lower expression levels of *TLR4*, while its expression levels in LAML (Acute Myeloid Leukemia), LGG (Brain Lower Grade Glioma), and PAAD (Pancreatic adenocarcinoma) were significantly higher, as shown in Figure 2F ($P < 0.05$).

A. Overall Survival (OS)



B. Disease Free Survival (DFS)

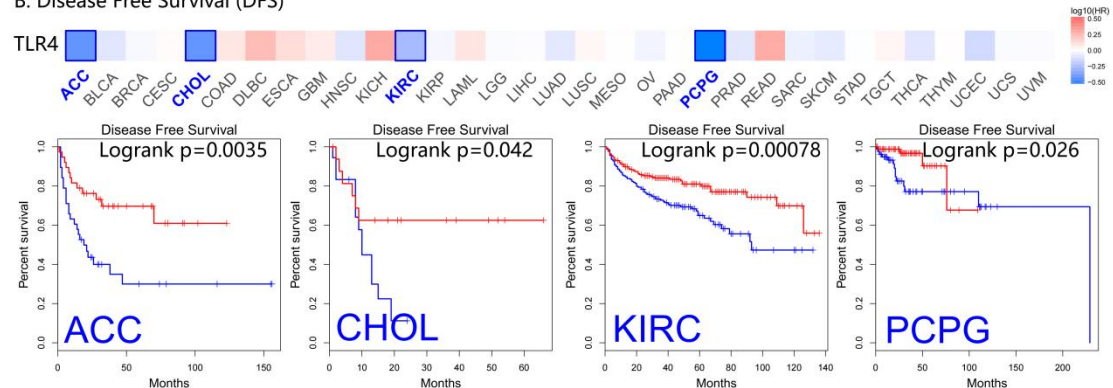


Figure 3 Survival analysis of *TLR4* in pan-cancer data obtained from the TCGA database. Survival analysis of *TLR4* on OS (A) and DFS (B) in pan-cancer, demonstrated using the survival map and plot. The prognostic potential of *TLR4* in predicting OS and DFS is displayed using the Kaplan-Meier Plotter. Log-rank $P < 0.05$ was considered statistically significant.

1.2 Prognostic potential of *TLR4*

The prognostic potential of *TLR4* in 33 cancer types, which were included in the TCGA database, was analyzed using Kaplan-Meier Plotter. *TLR4* showed significant potential in predicting OS (Figure 3A, $P < 0.05$) and DFS (Figure 3B, $P < 0.05$) in several tumor types. Elevated *TLR4* level was related to longer OS in KIRC, LUAD, and SKCM. Moreover, the overexpression of *TLR4* was related to prolonged DFS in ACC, CHOL, KIRC, and PCPG.

2. Comprehensive pan-cancer analysis of *TLR4* mutations

2.1 Mutant types of *TLR4*

The *TLR4* mutants were explored in pan-cancer using the cBioportal (Figure 4). The results showed a high mutation level with an alteration frequency of more than 10% in UCEC, SKCM, and LUAD (Figures 4A and 4B). The relationships of the *TLR4* mRNA expression levels and mutant types (Supplementary Figure S1) with CNAs (Supplementary Figure S2) were also analyzed. A total of 378 mutation sites, including 323 missenses, 49 truncating, and 6 splice site mutations, were found between amino acids 0 and 839 of *TLR4*, as shown in Figure 4D. The results showed the mutation site with the highest mutation frequency (E225) and the site with the highest mutation within the structural domain (G111) (Figure 4D). Six samples had mutations at the G111, including two cases of Lung Squamous Cell Carcinoma, two cases of Skin Cutaneous Melanoma, one case of Lung Adenocarcinoma, and one case of Head and Neck Squamous Cell Carcinoma.

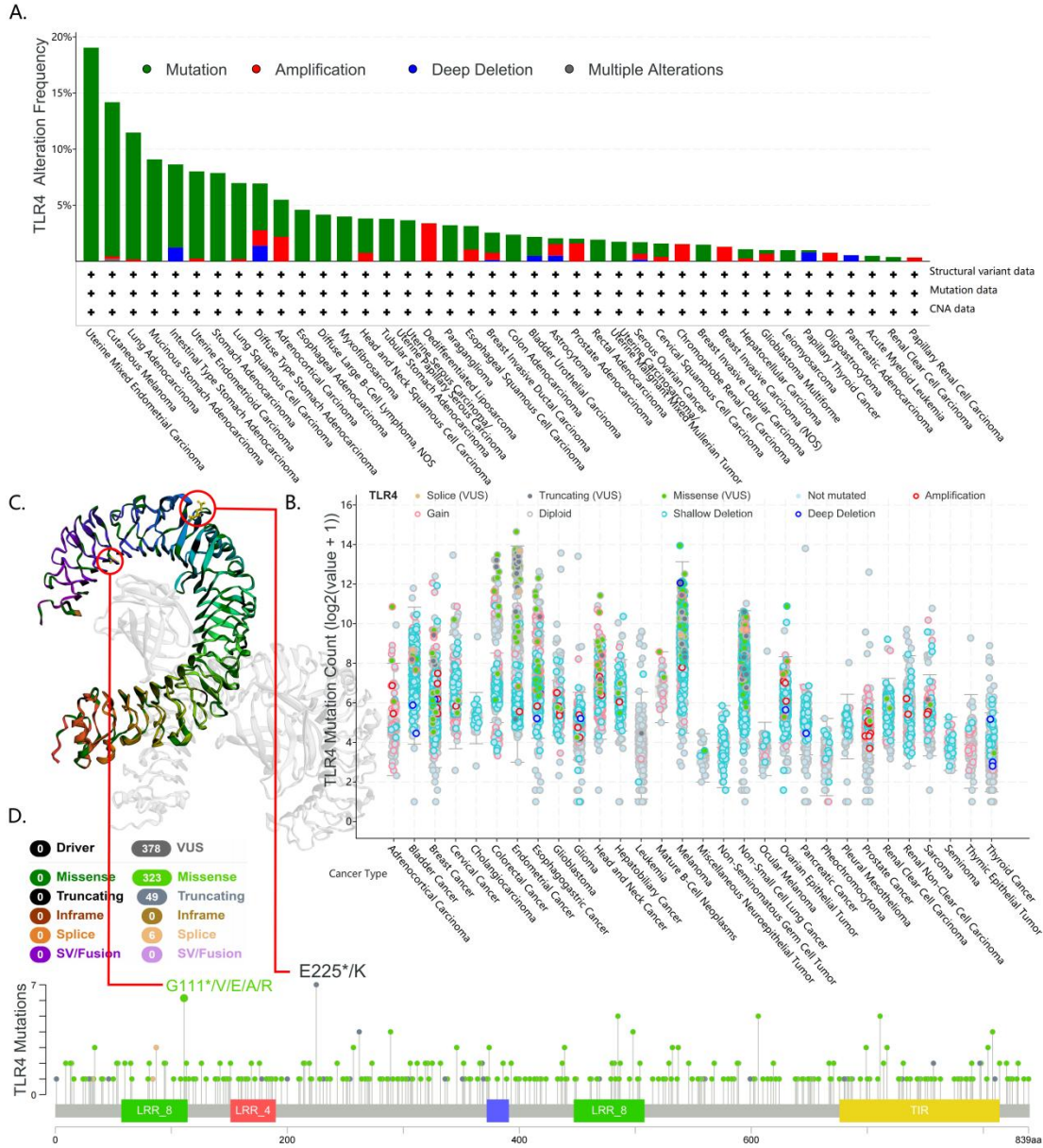


Figure 4 Mutation analysis of *TLR4* in pan-cancer using cBioportal database. The frequency of altered mutation types (A and B) and 3D structure (C) of *TLR4* in TCGA tumors are shown. The mutation site with the highest mutation frequency (E225) and the site with the highest mutation within the structural domain (G111) (D) are shown.

2.2 Pathway analysis of *TLR4*-mutant groups in cancer

All the tumor data obtained from the TCGA were divided into *TLR4* mutated and *TLR4* unmutated groups to detect the mechanistic effects of *TLR4* mutations on oncological progression in tumor patients. All the mutated genes in the two groups were analyzed differently using the KEGG (Kyoto Encyclopedia of Genes and Genomes) and GO (Gene ontology) pathways enrichment analyses. The most significantly enriched pathways, in which *TLR4* was directly

involved included cellular structural homeostasis, protein secretion, and other biological processes (Figure 5C). KEGG pathway enrichment analysis of the enriched genes revealed that the most significant differences were found in the *TLR4* mutant group for the pathways, such as the PI3K-AKT pathway, in which, *TLR4* was directly involved (Figure 5D).

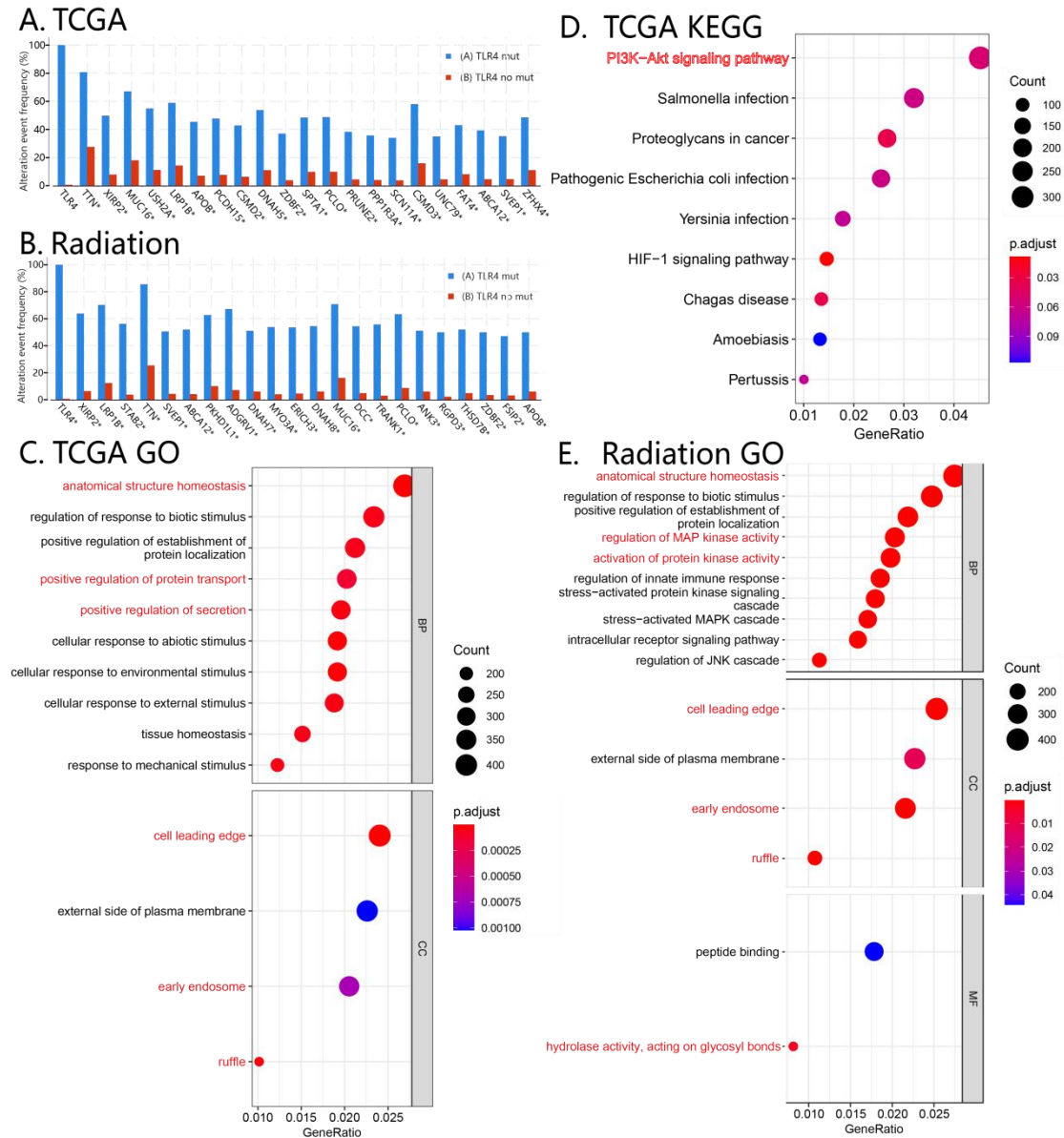


Figure 5 Enrichment analysis of *TLR4* mutation-related genes in cancer. By enriching for genes associated with *TLR4* mutations, the most significantly different genes are shown in bar charts (A) and analyzed for the KEGG pathway and GO pathway, with more significant differences indicating a higher frequency of mutations in this pathway and a relative reduction in pathway activity. The *TLR4*-enriched pathways are shown (C and D). Further analysis was performed on the *TLR4* mutant group in tumor patients treated with radiotherapy (B and E). $P < 0.05$.

The effects of *TLR4* mutations in 33 tumors from all the TCGA datasets were analyzed to identify the differentially expressed genes (DEGs) between the *TLR4* mutated and unmutated groups. The GO function enrichment analysis of the DEGs showed that they were involved in the regulation of GTPase activity, histone modification, cell-cell junction, and ion channel activity. KEGG pathway enrichment analysis of the DEGs showed that they were enriched in the calcium signaling pathway, HIF-1 signaling pathway, ECM-receptor interaction, and PI3K-Akt signaling pathway (Supplementary Figure S3).

TLR4 might act as an immune adjuvant to enhance the effects of radiotherapy-induced vaccines [20]. Therefore, the pathway alterations caused by *TLR4* mutations in patients treated with radiotherapy were further explored. It was observed that in *TLR4* mutant group, several protein kinase-related biological processes, such as MAP kinase activity, inner immune response, and the pathway of hydrolase molecules acting on glycosyl bonds, were significantly enriched (Figure 5E).

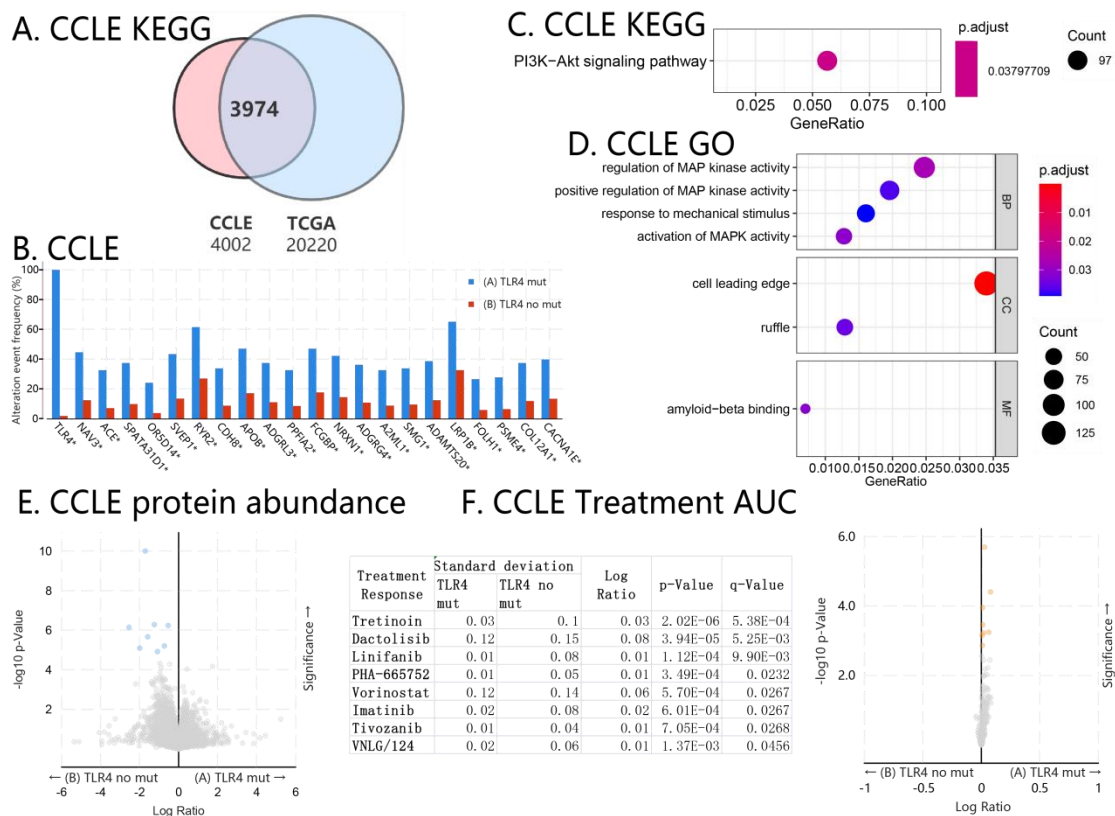


Figure 6 To determine the effect of *TLR4* mutation in tumor cells, we enriched the *TLR4* mutation group with differentially mutated genes in the CCLE database and intersected them with those enriched in the TCGA database (A). The most significant mutated genes between the two groups

are shown in bar graphs (B) and were analyzed using KEGG and GO pathway enrichment analyses (C and D).

The altered pathways associated with the *TLR4* mutant group in tumor cells were further analyzed to distinguish other cells, which were confused with the tumor cells. In tumor cells, MAP and MAPK-related pathways were mainly affected by *TLR4* mutations. The correlations among *TLR4* alterations, protein abundance, and treatment response were also analyzed using the CCLE database. The *TLR4* mutant groups showed a significant reduction in the expression levels of HNRNPUL1, OLFML2B, LCA5, C16ORF86, TPSAB1 DSG3, RNF223, and FST.

The tumor cell *TLR4* mutant group showed significantly higher therapeutic responses to Tretinoin (retinoic acid), Dactolisib (PI3K/mTOR inhibitor), Linifanib (RTK inhibitor), PHA-665752 (ATP-competitive c-Met inhibitor), Vorinostat (histone deacetylase, HDAC), Imatinib (protein tyrosine kinase inhibitor), Tivozanib (VEGFR inhibitor), and VNLG/124 and were significantly correlated with AUC (area under curve of ROC). These drugs are mainly targeted immunologic agents; therefore, further analysis of the *TLR4* role in the tumor immune microenvironment is needed.

2.3 Survival analysis of *TLR4*-mutant groups in cancer

The differences in survival and methylation alterations due to *TLR4* mutations in each cancer type were explored by analyzing the relationships between *TLR4* mutations and survival with the alterations in methylation using the data obtained from the TCGA database. Among the 33 cancer types in the TCGA database, the highest frequency of *TLR4* mutations was found in SKCM, LUAD, UCEC, LUSC, and STAD; all these had higher than 6% mutation frequency (Figure 7A). Survival analysis showed that *TLR4* mutations resulted in poor OS and DFS of ESCA (Esophageal carcinoma) and poor DFS of HNSC (Head and Neck squamous cell carcinoma) (Figure 7B). Both the ESCA and HNSC tumors are solid tumors; therefore, the correlations between *TLR4* mutations and PFS in the MSS Mixed Solid Tumors data, which incorporated 249 mixed solid tumors and matching normal tissue from patients, were analyzed [9]. It was found that *TLR4* mutations resulted in significantly poor PFS (Figure 7C).

2.4 Methylation analysis of *TLR4*-mutant groups in cancer

The differences in methylation levels between the *TLR4* mutated and unmutated groups were analyzed, and only data from cancer types with six and more patients in the *TLR4* mutated group

were included. The results showed that in the *TLR4* mutation group, the methylation burden was reduced in all nine cancer types except BLCA and UCEC (Figure 7D).

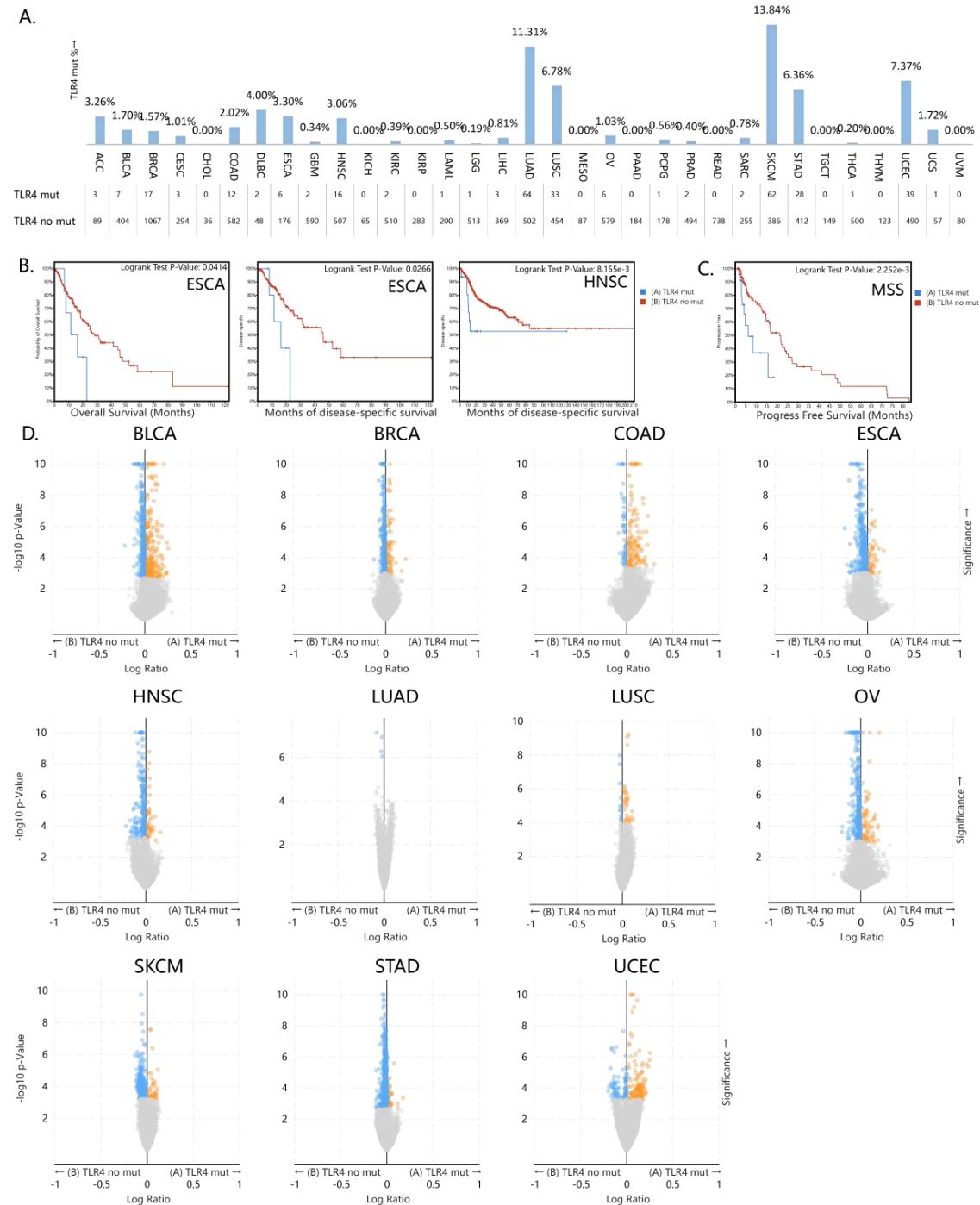


Figure 7 Effects of *TLR4* mutations on the survival and gene methylation levels in various cancer types. The percentage and number of *TLR4* mutations in 33 tumor types were analyzed using the TCGA database (A). *TLR4* mutation significantly reduced the OS and DFS of ESCA and DFS of HNSC (B). Data from MSS Mixed Solid Tumors (Broad/Dana-Farber, Nat Genet 2018) revealed

that *TLR4* mutations reduced PFS in tumor patients (C). The methylation levels in the 11 cancer types with the number of *TLR4* mutation cases >6 in the TCGA database are listed separately (D).

2. 5 Altered CNV of *TLR4* in relation to immune cells infiltration

The relationship between alteration in the CNVs of *TLR4* and immune cell infiltration in tumor tissues was analyzed. The results showed that differences in *TLR4* mutations and *TLR4* mutation types in CNV data caused differences in some tumor-infiltrating immune cells (Figure 8). The remaining data on the correlations between *TLR4* mutations and immune cell infiltration in tumor tissues are listed in Supplementary Table S2 and Figure S4. Moreover, the relationship between *TLR4* expression and infiltration of CD8+ T cells and macrophages in tumor tissues was also analyzed. The results were similar to those of the other studies, suggesting that *TLR4* expression was positively correlated with both CD8+ T cell and macrophage infiltration scores in tumors (Supplementary Figure S6).

The classical studies suggested that *TLR4* was mainly expressed in the immune cells of myeloid origin and expressed on macrophages to recognize LPS or endogenous ligands, such as biglycan, HMGB1, S100A8, and S100A9, during the immune response or cancer metastasis. Therefore, the first step in this study was to analyze the correlation between *TLR4* mutations and macrophage infiltration in tumors. It was found that *TLR4* mutations in UCEC could lead to increased infiltration of macrophages (both M1 and M2-type), as shown in Figure 8A. In PRAD (Prostate adenocarcinoma), *TLR4* mutations resulted in a significant decrease in the macrophage/monocyte ratio and a significant increase in M1-type macrophage infiltration in LUSC, HPV+ HNSC, COAD, BRCA-LumB, and, BRCA while significantly decreasing the M0-type macrophage infiltration in HPV-HNSC and ESCA. Different types of CNV alterations could also lead to significant differences in macrophage infiltration (Figure 9). In BRCA, M0 macrophage infiltration was much higher in the high application mutation group than that in the normal group and other mutation types, while M2 macrophage infiltration was the lowest. Moreover, in BRCA-Her2 and HNSC, the high application mutation group had the lowest, while it was the highest in the PRAD.

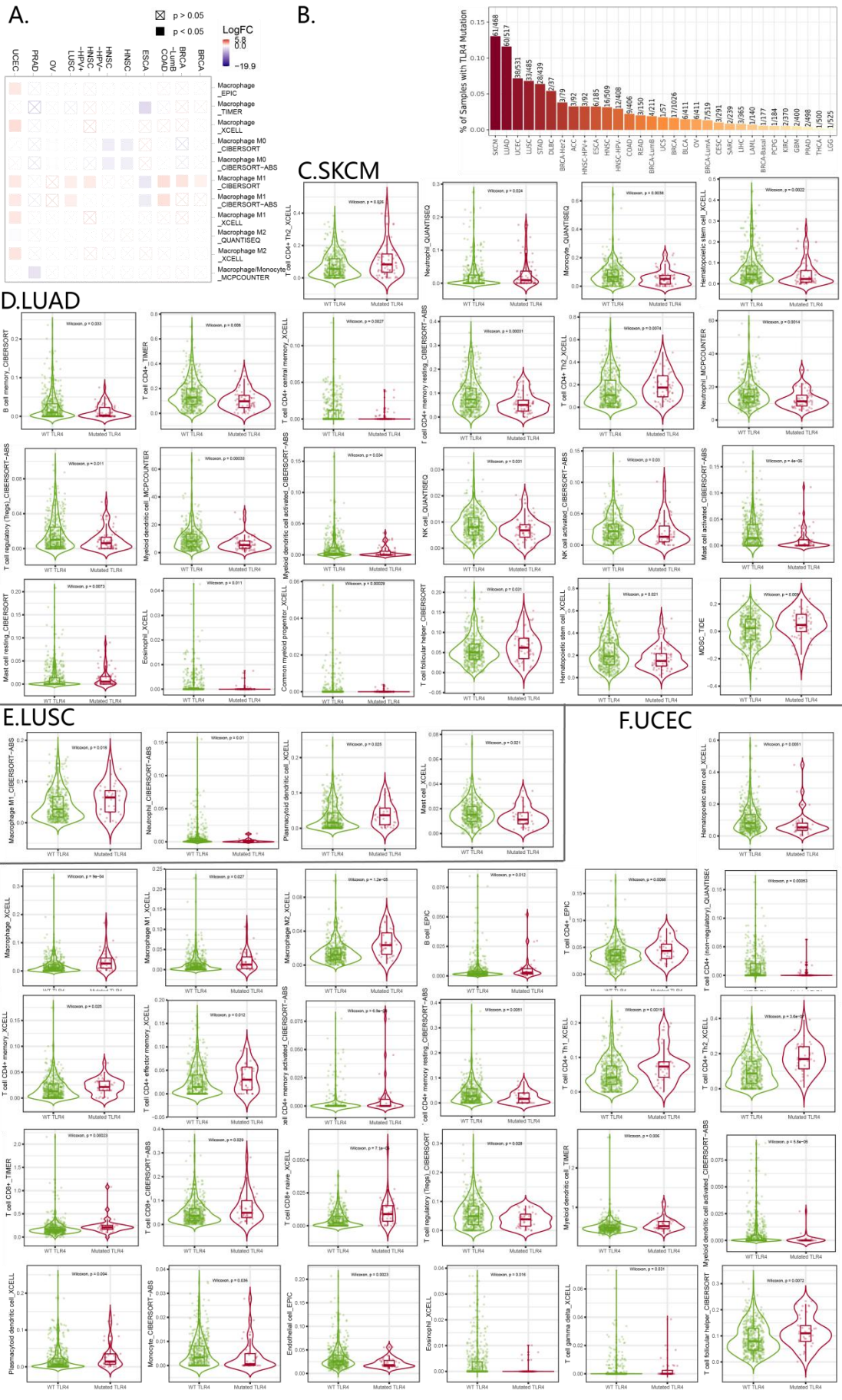


Figure 8 (A) Differential tumor immuno-infiltration level in cancer by *TLR4* mutant. (B) The frequency of *TLR4* gene mutations in tumors. (C-F) Among the four tumors with the highest frequency of *TLR4* gene mutations, tumor immuno-infiltration level in cancer by *TLR4* mutant.

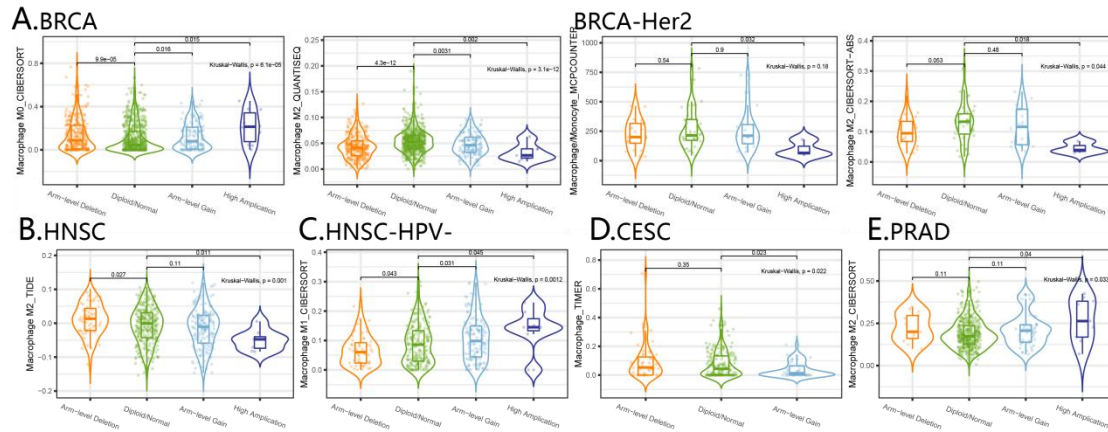


Figure 9 Compare immune infiltration distribution by the sCNA status of *TLR4* across TCGA cancer types (A-E). Estimation of sCNA information from copy number segmentation profiles at the gene level, including “deep deletion”, “arm-level deletion”, “diploid/normal”, “arm-level gain”, and “high amplification” defined by GISTIC2.0.

3. Immunotherapy response based on *TLR4* expression

The correlation between *TLR4* expression and therapy outcome in the clinical studies of immune checkpoint blockade (ICB) therapy was analyzed (Figure 10). Moreover, the Pearson correlation between *TLR4* expression and cytotoxic T lymphocyte level was also analyzed using TIDE [19] (Supplementary Table S3). The relationship between *TLR4* expression and tumor immune cell infiltration was also analyzed. *TLR4* expression was positively correlated with CD8+ T cell and macrophage infiltration scores, particularly with M2 macrophage immune infiltration scores, in most tumors. The macrophage/monocyte ratio, calculated using MCP-CUNTER, was also significantly positively correlated (Supplementary Figure S4). It is important to note that *TLR4* expression is always positively correlated with the infiltration level of cytotoxic T lymphocytes; however, there are differences in the relationship between *TLR4* expression and tumor prognosis in different studies. The patients treated with anti-PD1, anti-CTLA4, ICB, and combined anti-PD1+anti-CTLA4 showed better OS and PFS in the high *TLR4* expression group (except for Braun's study in Kidney clear patients, where *TLR4* expression had a non-significant effect on PFS). However, high *TLR4* expression tended to lead to poor OS and PFS (statistically

insignificant) in patients treated with anti-PDL1 and ACT. Thus, in the overall immunotherapy against both PD1 and CTLA4 immune checkpoints, *TLR4* expression levels were significantly associated with prognosis.

A. OS

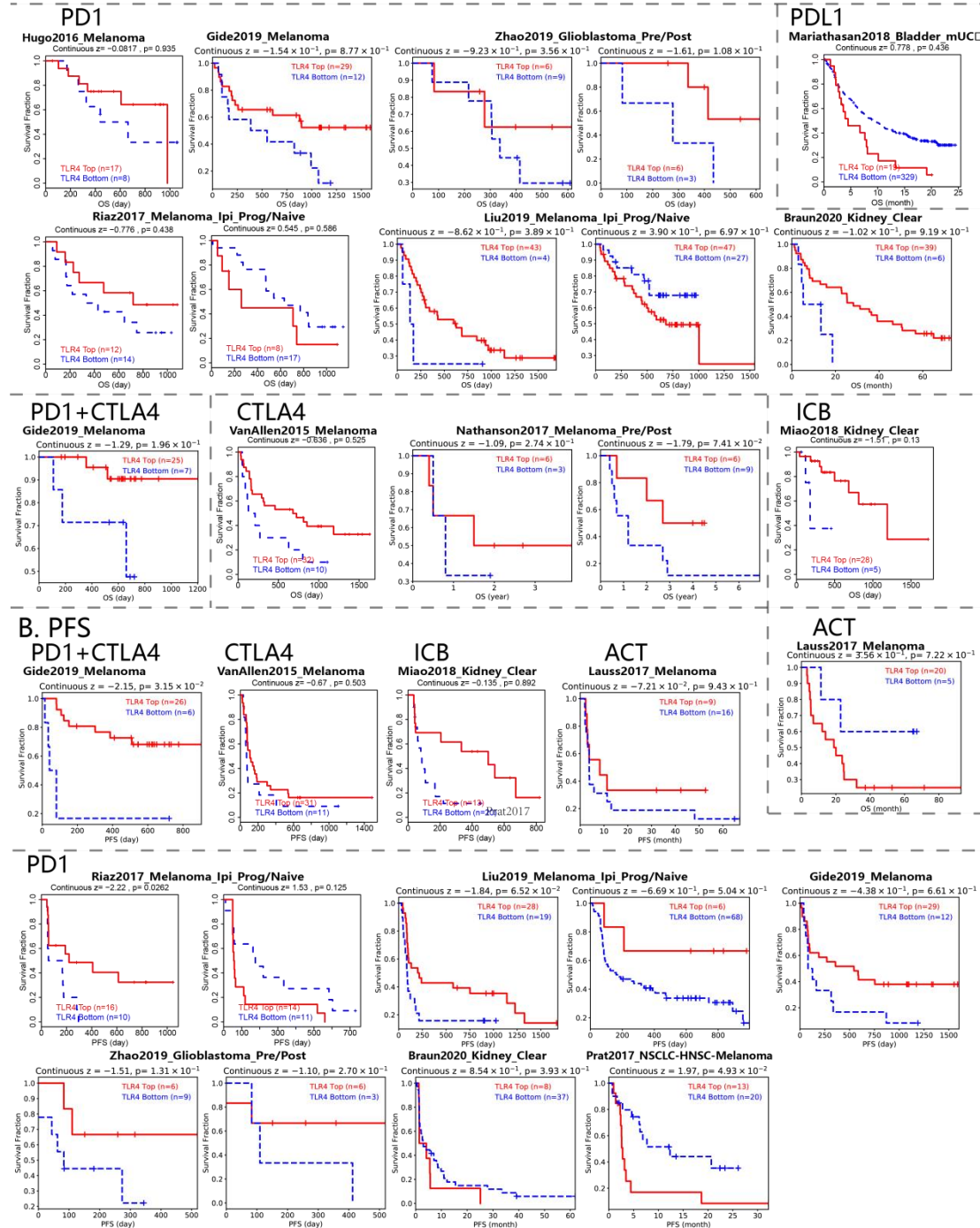


Figure 10 A correlation between *TLR4* expression and ICB therapy outcomes in ICB clinical trial studies is shown. Survival risk score: z-score of *TLR4* gene effect on death risk in CoxPH model.

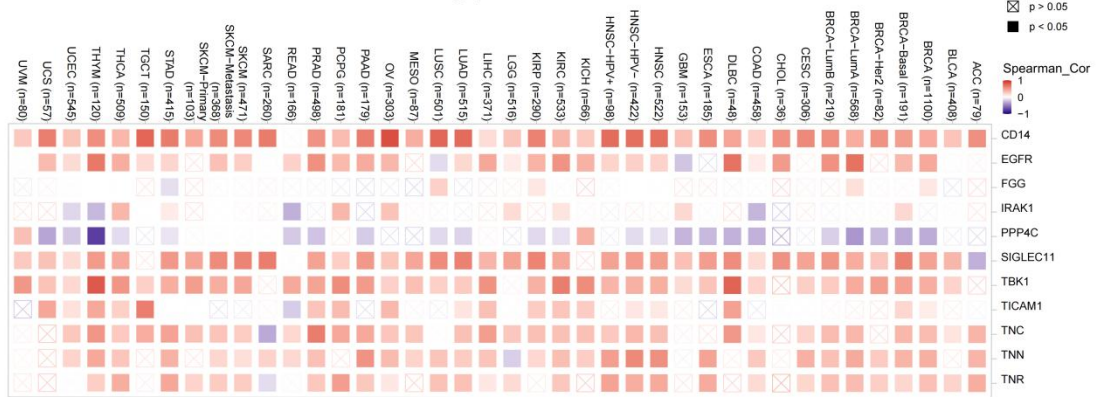
4. Pan-cancer analysis of *TLR4*-related genes

The proteins interacting with *TLR4* protein (PPI) were analyzed using the STRING database. A total of 50 experimentally validated interacting proteins with an interaction score of 0.150 and 11 genes (*CD14*, *EGFR*, *FGG*, *IRAK1*, *PPP4C*, *SIGLEC11*, *TBK1*, *TICAM1*, *TNC*, *TNN*, and *TNR*) out of 3974 genes with mutational differences associated with *TLR4* mutations in tumor tissues and tumor cells were screened. The correlation between *TLR4* and the expression of these 11 genes in 33 tumor types was systematically analyzed. *TLR4* was found to be significantly and positively correlated with the expression of all the genes except *PPP4C* (Figure 11A). Moreover, the correlation between the expression levels of these genes set and the prognosis in each cancer type was analyzed (Supplementary Figure S5).

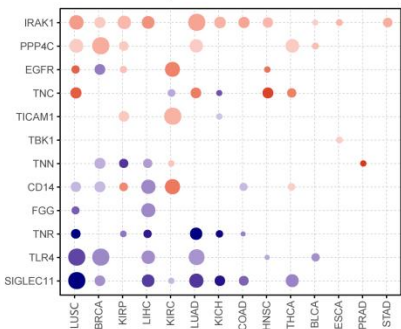
4. 1 Expression and SNV analysis of *TLR4*-related genes

Differences in the expression of these 12 genes in tumor and normal tissues, correlations between expression and survival, and expression in the different subtypes were then systematically analyzed (Figures 11B-11D). The relationship between the expression of each gene and the survival of tumor patients is shown in Supplementary Figure S5. Moreover, the frequency of SNVs in the 12 genes in different tumor types was also analyzed (Figure 11E). The relationship between these gene mutations and survival was analyzed based on SNVs, and the results showed that only the *EGFR* mutation group in LGG and LUAD showed significantly better overall survival (Figure 11F). In the TCGA database, the frequency of mutations in *CD14* and *PPP4C* genes was less than 1%, and the distribution of mutations in the other 10 genes is shown in Figure 11H. The mutation type and proportion of the target gene list in two lung cancer types are shown in the waterfall plot, where the highest mutation frequencies were in *TNR*, *TNN*, *TLR4*, and *EGFR*. The highest mutation types were missense and nonsense mutations; in *EGFR*, in-frame del accounted for 1/3 of the total *EGFR* mutations.

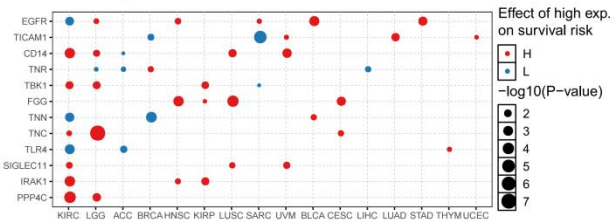
A. Correlation between TLR4 and Interacting proteins



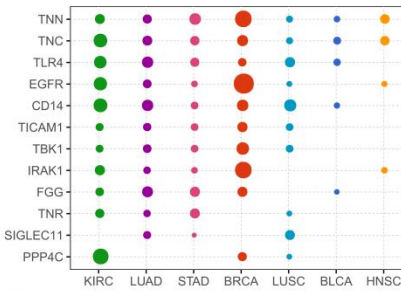
B. Differential Expression-Tumor vs. Normal



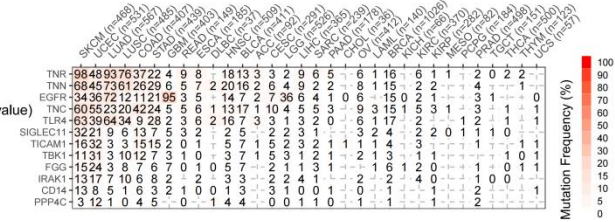
C. Expression Survival



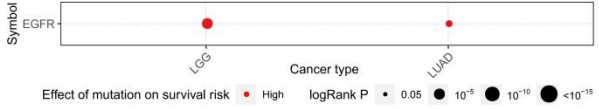
D. Expression Subtype



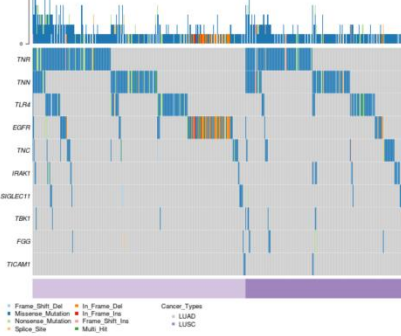
E. SNV frequency



F. OS between mut and non-mut genes.



G. mutation distribution in lung cancer



H. mutation distribution in 33 cancer

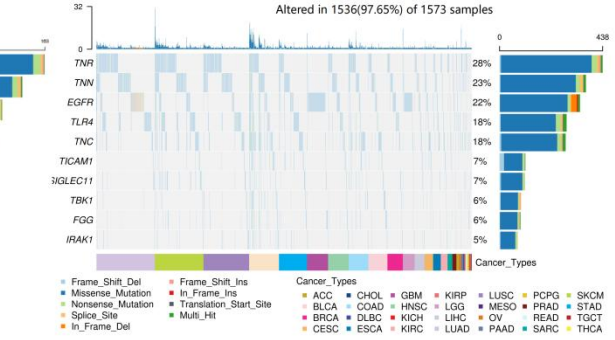


Figure 11 *TLR4*-related gene expression and SNV analysis. (A) Correlation of *TLR4* expression with 11 related genes in 33 tumors. (B) The color from purple to red represents the fold change between the tumor vs. normal. The size dot indicates the significance. The dot was filtered based on the fold change (FC >2) and significance (FDR < 0.05). (C) The dot represents the gene effects on the survival of the cancer types; the p-value is the Kaplan Meier *P*-value. The dot color

indicates the worse of the high (red) or low (blue) expression in the cancer types. (D) Figure represents the effects of genes on subtypes. (E) SNV frequency of genes in each cancer. The deeper the color, the higher the mutation frequency. Numbers in each cell represent the number of samples with the corresponding mutated genes in corresponding cancers. The 0 and blank in the cell indicated no mutation in the coding region of the gene and no mutation in all regions, respectively. (F) Survival differences between mutant and non-mutant genes are shown only for genes with significant *P*-values ($< \text{ or } = 0.05$). (G-H) Mutation distribution of mutated genes and classification of SNV types, including missense mutation, frameshift deletion, nonsense mutation, etc. in lung cancer and all tumors. The sidebar graph and top bar graph show the number of mutations in each sample or each gene.

4.2 CNVs analysis of *TLR4*-related genes

Different genes have different CNVs in each type of cancer; therefore, the CNVs of these genes in 32 tumors were analyzed (Figure 12A). The results revealed that ESCA, LUAD, LUSC, and UCS exhibited higher CNVs. *EGFR*, *TNN*, and *TNR* genes had the highest frequency of CNVs, such as SNV, in tumors. The types of CNVs in these 12 genes, which were associated with *TLR4*, were dominated by heterozygous amplification and deletion. Therefore, the *TLR4*-related genes in each tumor type for by the heterozygous amplification and deletion mutations were further analyzed (Figure 12B). Moreover, as gene expression is often affected by CNVs, the correlations between mRNA expression and CNV frequency in different tumors were analyzed (Figure 12C). It was found that the higher the frequency of CNVs in these genes, the higher the mRNA expression. *TBK1*, *PPP4C*, *TICAM1*, and *EGFR* showed the highest correlation between their mRNA expression levels and CNVs in tumors. However, *TLR4* in ACC and *TNR* in PAAD had the opposite mRNA expression levels and CNVs frequency. The present study further analyzed the effects of genes with CNVs on pathway activation/inhibition in 32 tumor ratios, as shown in Figure 12D. Consequently, the genes, whose expressions were significantly regulated by CNV, were obtained. It was found that CNVs in *TLR4*, *TBK1*, *SIGLEC11*, *PPP4K*, *IRAK1*, and *CD14* activated the apoptosis pathway in most tumor types, while those in *TNN*, *TNC*, *TLR4*, *TICAM1*, *SIGLEC11*, *EGFR*, and *CD14* activated the EMT pathway. Moreover, the CNVs in *TNN*, *TNC*, *TLR4*, *TICAM1*, *EGFR*, and *CD14* inhibited the cell cycle pathway in most tumor types, and those

in *PPP4C* and *IRAK1* activated the cell cycle pathway in most tumors. Similarly, the percentage of cancers activated/repressed by the CNVs of these genes for each pathway is shown in a heat map (Figure 12E).

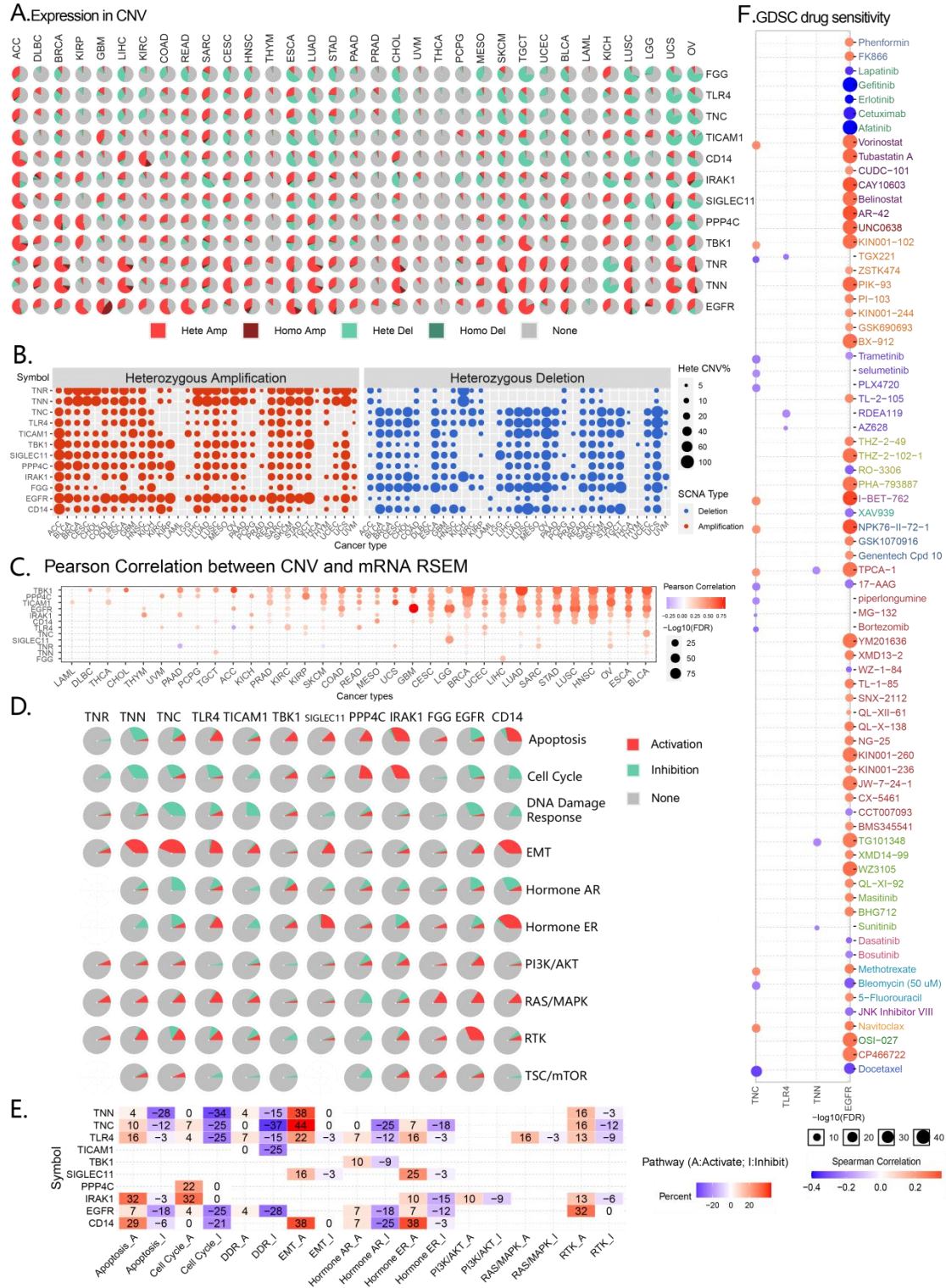


Figure 12 CNVs analysis of TLR4-related genes. (A) CNVs of each gene in each cancer helped in analyzing the expression of genes, which were significantly affected by CNVs. Hete Amp:

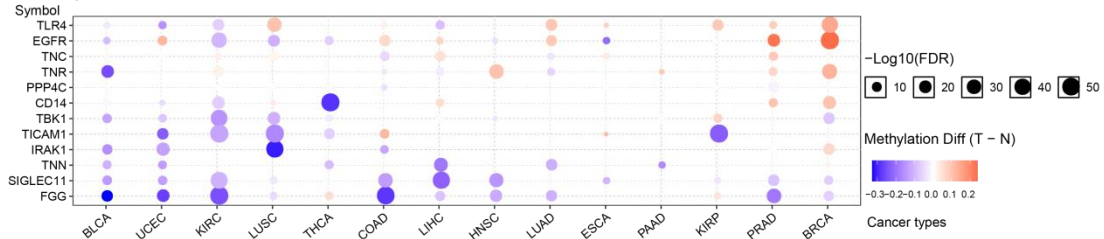
heterozygous amplification; Hete Del: heterozygous deletion; Homo Amp: homozygous amplification; Homo Del: homozygous deletion; None: no CNV. (B) Heterozygous CNV profile showed the percentage of heterozygous CNV, including amplification and deletion percentage of heterozygous CNVs in each gene in each cancer type. (C) Genes, whose mRNA expression levels were significantly ($FDR \leq 0.05$) correlated with CNVs percentage, are shown in the Figure. Blue bubbles represent a negative correlation (when a gene has a high CNV frequency, the gene expression downregulates, and they have an opposite trend), and red bubbles represent a positive correlation; the deeper the color, the higher the correlation. (D) Global percentage of cancers in which a gene affects the pathway in different cancers, showing percentage (number of activated or inhibited cancer types/32 *100%). (E) Heatmap, showing genes that have a function (inhibition or activation) in at least 5 cancer types. Pathway_a (red) represents the percentage of cancers, in which a pathway might be activated by genes, and pathway_i (blue) represents the percentage of cancers, in which a pathway might be inhibited by genes. (F) The gene set drug resistance analysis using GDSC IC50 drug data. The Spearman correlation represents the correlations of gene expression with the drugs. The positive correlation means that the high expression of the gene was resistant to the drug, and vice versa.

Furthermore, the drug sensitivity of *TLR4*-related genes in the GDSC database was analyzed using the GSCALite tool. The high *TLR4* expression was correlated with higher sensitivity to TGX-221 (PI3K inhibitor), RDEA119 (Refametinib, MEK inhibitor), and AZ628 (Raf inhibitor). The details of elevated *TNN*, *TNC*, and *EGFR* expression in response to drug sensitivity or resistance are shown in Figure 12F.

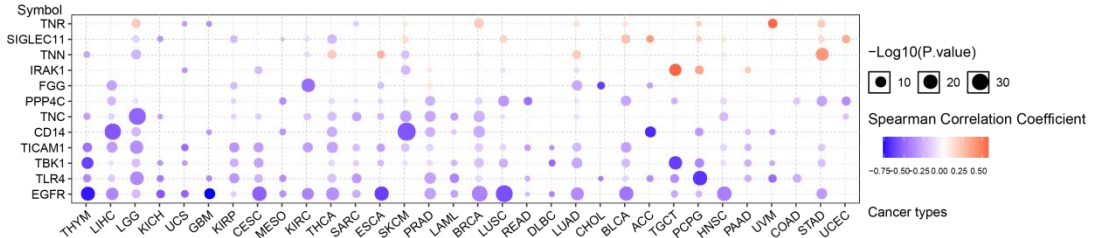
4.3 Methylation analysis of *TLR4*-related genes

Previous results showed that the *TLR4* expression in individual tumors resulted in significant differences in methylation. Therefore, a pan-cancer analysis of methylations in *TLR4*-related genes, including the differences in methylation levels of *TLR4*-related genes in different tumors and corresponding normal tissues, their effects on overall survival, and correlations between gene expression and methylation levels, was performed further (Figure 13A-13C).

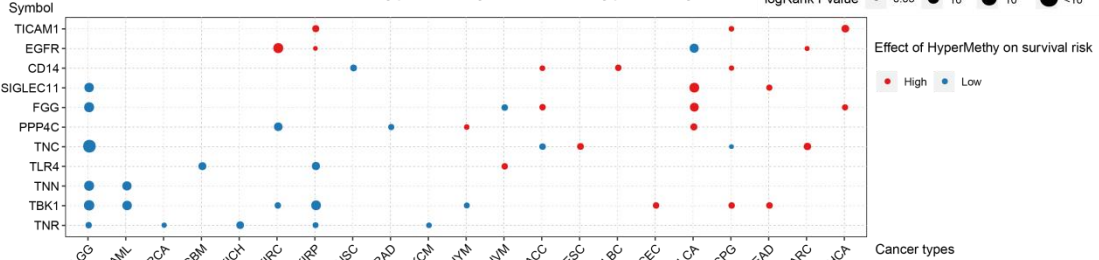
A. Methylation difference between tumor and normal samples.



B. Spearman Correlation Coefficient of methylation and gene expression.



C. Overall survival difference between hypermethylation and hypomethylation.



D. Top TLR4-related genes in immuno-oncology experiments

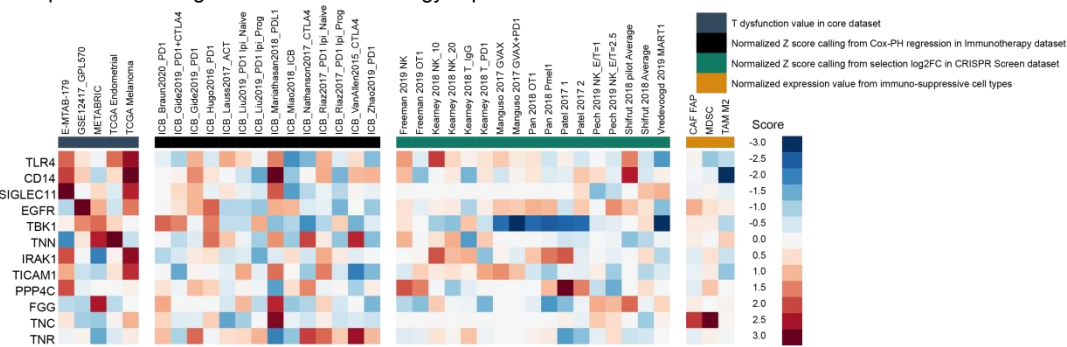


Figure 13 Methylation analysis of TLR4-related genes. (A) Differential methylation bubble plot, showing changes in the methylation patterns in genes between tumor and normal samples in each cancer. Blue color represents a methylation downregulation in tumors and vice versa for the red color. (B) Pearson correlation between methylation and mRNA expression levels. The blue color represents a negative correlation (means when the level of gene methylation upregulates, the gene expression downregulates, showing the opposite trend), and the red color represents a positive correlation; the deeper of color, the higher the correlation. (C) Survival differences between the samples with hypermethylated and hypomethylated genes are shown in the figure only for genes with significant log-rank P -values (≤ 0.05). Red color represents the worse results of the high methylation group, and vice versa for the blue color. The size of the point represents statistical

significance, the bigger the size, the more significant it is. (D) *TLR4*-related genes validated in different tumor immunology assays were derived from four aspects. Genes (row) are ranked by their weighted average value across four immunosuppressive indices (columns), including T cell dysfunction score, T cell exclusion score, association with ICB survival outcome, and log-FC in CRISPR screens. The T dysfunction score shows how a gene interacts with cytotoxic T cells to affect the patient survival outcomes, and the T cell exclusion score assesses the gene expression levels in immunosuppressive cell types, which drive T cell exclusion. The association score (z-score in the Cox-PH regression) of ICB survival outcome evaluates the genes, whose activities are correlated with ICB benefit. The normalized log-FC in CRISPR screens helps in identifying regulators, whose knockout can mediate the efficacy of lymphocyte-mediated tumor killing in cancer models.

4. 4 Immuno-oncology analysis of *TLR4*-related genes

The potential of *TLR4*-related genes in the immune-oncology was explored, and the potential mechanisms of the 12 genes in tumor immunity, which had been experimentally validated, were analyzed. The *TLR4*-related genes were prioritized for the next steps in tumor immune mechanisms using the Regulator Prioritization module of TIDE [19]. The results were evaluated for each gene for the correlations of their expression levels with ICB response outcome, T cell dysfunction levels, T cell exclusion levels, and phenotypes in genetic screens in diverse cohorts (Figure 13D). The results revealed that *CD14* expression was lowest in the immunosuppressed cells and TAM M2, while *TNC* expression was the highest in MDSC immunosuppressed cells. However, the most relevant gene for the activation of cytotoxic T-cells in the five core datasets was *TLR4* and its ligand *CD14*. In Mariathasan 2018_PDL1 study [21], in which ICB treatment was studied, *CD14* activity was significantly positively correlated with ICB benefit, and *TLR4* in the Kearney 2018 NK_20 was involved in regulating lymphocyte-mediated tumor-killing potency in tumor models.

Discussion

TLR4, an important member of the immunoglobulin superfamily, is involved in several physiological and pathological processes, including lymphocyte response and cell adhesion. It has been suggested that *TLR4* is closely associated with tumorigenesis and metastasis [22,23]. Fleming et al. recently reported that tumor cell-derived extracellular vesicles regulated the expression of

PD-L1 via *TLR4* signaling, thereby converting normal myeloid cells into functional MDSCs [24]. *TLR4*-induced TGF- β expression was also correlated with the conversion of fibroblasts to cancer-associated fibroblasts (CAF) in the TME, thereby promoting the proliferation and growth of cancer cells [24,25]. The S100A8-induced inflammatory cytokines/chemokines in a *TLR4*-dependent manner and anti-S100A8 neutralizing antibodies could also inhibit tumor progression by inhibiting the recruitment of MDSCs [26]. Deguchi's unpublished data reported that the neutralizing antibodies inhibited both pulmonary and hepatic metastases [22]. Tumors could block the priming of *TLR4* by expressing ligands, thereby shaping a metastasis-friendly TME.

In the current study, the expression levels and mutant status of *TLR4* in pan-cancer were explored. *TLR4* levels significantly decreased in tumor tissues as compared to those in the normal tissues in most cancers and were closely related to the patient's survival outcomes. The results of the current and previous studies showed the excellent predictive potential of *TLR4* in various cancers.

Clinical and genomic data were systematically collected and integrated to assess the correlations between the different mutational statuses of *TLR4*, other genetic mutations, methylation levels, survival, and clinical characteristics of cancer patients. The results showed that the *TLR4* mutation group exhibited a better prognosis in solid tumors. The mutated genes associated with *TLR4* mutations were mainly enriched in the PI3K-AKT pathway and were directly involved in cellular structural homeostasis, protein secretion, and other biological processes, which were consistent with previous studies [27,28,29]. *TLR4* might act as an immune adjuvant to enhance the effects of radiotherapy-induced vaccines [20]. Enrichment analyses showed that several mutated genes associated with MAP protein kinase and biological process pathways related to endogenous immune activation were enriched in patients treated with radiotherapy in the *TLR4* mutant group. The activation of *TLR4* induced endogenous immunity using the MAP pathway, which stimulated the transcription of cytokine genes [30]. This might be a potential pathway for radiotherapy to activate the tumor immune microenvironment via the *TLR4*/MAP pathway, which indicated a potential direction for the further combination of radiotherapy with immunotherapy.

Moreover, the sensitivity of tumor cells with *TLR4* mutations to the currently developed targeted drugs was also analyzed. The results showed a significantly higher sensitivity of eight

targeted drugs, including Dactolisib (PI3K/mTOR inhibitor), Linifanib (RTK inhibitor), PHA-665752 (ATP-competitive c-Met inhibitor), Vorinostat (histone deacetylase, HDAC), Imatinib (protein tyrosine kinase inhibitor), and Tivozanib (VEGFR inhibitor).

In addition to SNVs, the CNAs were also an important mechanism in tumors, where *TLR4* exerted an immune role in close association with macrophages. However, no studies were conducted on the effects of *TLR4* CNVs on the infiltration of macrophages in the TME. Therefore, in the current study, the effects of *TLR4* gene CNVs on the infiltration of tumor immune cells in several tumors with the highest frequency of CNVs were preliminarily analyzed. The results revealed that *TLR4* mutations caused a significant increase in the infiltration of M1-type macrophages in LUSC, HPV+HNSC, COAD, BRCA-LumB, and BRCA. In contrast, in the HPV-HNSC and ESCA, the *TLR4* mutations led to a significant decrease in the infiltration of M0 and M1 macrophages, respectively. Furthermore, the High Application group was significantly negatively correlated with the infiltration of M2-type macrophages in BRCA and HNSC and vice versa for PRAD. This finding indicated a way for the further differentiation of *TLR4* in regulating TME in different tumors.

The correlations between the expression levels of the *TLR4* gene with its mutational status, clinical outcomes, and levels of immune cell infiltration in patients with different cancer types were comprehensively analyzed for the first time in the current study. Previous studies analyzed the relationship between *TLR4* expression, patient prognosis, and immune cell infiltration in pan-cancer. The results showed that *TLR4* expression was associated with the prognosis of patients with KIRC, SKCM, STAD, TGCT, and UCEC as well as with the infiltration levels of CD4 and CD8 T cells, macrophages, neutrophils, and dendritic cells [31]. Based on the mutational profile of *TLR4*, this study further analyzed the role of *TLR4* in the prognosis of immunotherapy. The results found that *TLR4* was associated with a better prognosis for immunotherapy, such as PD-1 and CTLA4. The previous studies showed that PD-1 resistance was due to the activation of the *TLR4* pathway, triggering an inflammatory response, which further corroborated the current findings [32,33].

Among the total 3974 genes screened in tumor tissues and cells, which were differentially associated with *TLR4* mutations, 11 genes (*CD14*, *EGFR*, *FGG*, *IRAK1*, *PPP4C*, *SIGLEC11*, *TBK1*, *TICAM1*, *TNC*, *TNN*, and *TNR*) showed direct protein-functional correlations with *TLR4*

and were further analyzed in terms of the functions caused by the mutations. The results revealed that these genes were mainly involved in biological processes, such as apoptosis, cell cycle, DNA damage response, and EMT, and were closely related to PI3K/AKT, RAS/MAPK, and RTK signaling pathways. Moreover, their different expression and mutation in each cancer species were also closely related to tumor prognosis. These genes were ranked according to an immunosuppressive index to further explore the next experimental direction. The index consisted of T-cell dysfunction/rejection scores, association with ICB survival outcomes, and log FC in CRISPR screens. The results showed that *TLR4* and its ligand CD14 were significantly and positively correlated with immunocidal capacity in five cancer datasets. Several studies found that tumor-infiltrating lymphocytes, known as TAMs, could affect the prognosis and effectiveness of chemotherapy and immunotherapy [1,2]. The results showed that *TLR4* and its ligand CD14 were significantly and negatively associated with the immunosuppressed MDSCs and TAM M2. Our previous studies also verified that activating the *TLR4* pathway could promote macrophage polarization towards M1 [34]. This result was further validated in the current study from a bioinformatics perspective, which found that the potential varied in different cancers.

Conclusions

The expression levels of *TLR4* were significantly lower in tumors than those in normal tissues in most cancer types and were strongly associated with patient outcomes. The mutated genes associated with *TLR4* mutations were mainly enriched in the PI3K-AKT pathway. This could be a potential pathway for radiotherapy to activate the tumor immune microenvironment via *TLR4*/MAP, which indicated a potential direction for the combination of radiotherapy with immunotherapy. In tumors, *TLR4* mutations were closely associated with the M1/M2 polarization of macrophages. *TLR4* and its ligand CD14 were significantly and negatively associated with immunosuppressed MDSCs and TAM M2. Thus, the intervention of *TLR4*-dependent signaling pathways might be a promising strategy to reduce tolerance to ICB treatment in the post-immune era. Briefly, the prognostic potential and immune aspects of *TLR4* in pan-cancer were comprehensively explored, revealing its pivotal role in immuno-oncology. However, the lack of functional and mechanistic studies at the cellular and immunological levels was the major limitation of the current study. Therefore, more in-depth functional and mechanistic studies are further needed.

Acknowledgements

The authors would like to thank all the reviewers who participated in the review, as well as MJEditor (www.mjeditor.com) for providing English editing services during the preparation of this manuscript.

Authors' contributions

Yuan Wang has done the most bioinformatics analysis and written manuscripts. Lehui Du, Pei Zhang, Xingdong Guo and Na Ma did the perspective and conclusion parts. Qian Zhang, Yan Wang and Xiang Huang did the data analysis. Xin Tan, Jiangyue Lu, Qingchao Shang and Yanan Han did the background research. Xiao Lei and Baolin Qu participated in the writing of paper and revision of manuscript. All authors read and approved the final manuscript.

Funding

Not applicable.

Availability of data and materials

The datasets are available under reasonable request.

Ethics approval and consent to participate

Not applicable.

Consent for publication

Not applicable.

Conflict of Interest statement

The authors declare that they have no competing interests.

Reference

- [1] Siegel RL, Miller KD, Fuchs HE, et al. Cancer statistics, 2022. *CA Cancer J Clin.* 2022 Jan;72(1):7-33.
- [2] Rahib L, Wehner MR, Matrisian LM, et al. Estimated Projection of US Cancer Incidence and Death to 2040. *JAMA Netw Open.* 2021 Apr 1;4(4):e214708.
- [3] Hanahan D. Hallmarks of Cancer: New Dimensions. *Cancer Discov.* 2022 Jan;12(1):31-46.

- [4] Combes AJ, Samad B, Tsui J, et al. Discovering dominant tumor immune archetypes in a pan-cancer census. *Cell*. 2022 Jan 6;185(1):184-203. e19.
- [5] Alvarado AG, Thiagarajan PS, Mulkearns-Hubert EE, et al. Glioblastoma Cancer Stem Cells Evade Innate Immune Suppression of Self-Renewal through Reduced TLR4 Expression. *Cell Stem Cell*. 2017 Apr 6;20(4):450-461. e4.
- [6] Kirtland ME, Tsitoura DC, Durham SR, et al. Toll-Like Receptor Agonists as Adjuvants for Allergen Immunotherapy. *Front Immunol*. 2020 Nov 12;11:599083.
- [7] Zheng JH, Nguyen VH, Jiang SN, et al. Two-step enhanced cancer immunotherapy with engineered *Salmonella typhimurium* secreting heterologous flagellin. *Sci Transl Med*. 2017 Feb 8;9(376):eaak9537.
- [8] Guo X, Du L, Ma N, et al. Monophosphoryl lipid A ameliorates radiation-induced lung injury by promoting the polarization of macrophages to the M1 phenotype. *J Transl Med*. 2022 Dec 14;20(1):597.
- [9] Miao D, Margolis CA, Vokes NI, et al. Genomic correlates of response to immune checkpoint blockade in microsatellite-stable solid tumors. *Nat Genet*. 2018 Sep;50(9):1271-1281.
- [10] Goldman MJ, Craft B, Hastie M, et al. Visualizing and interpreting cancer genomics data via the Xena platform. *Nat Biotechnol*. 2020 Jun;38(6):675-678.
- [11] Nusinow DP, Szpyt J, Ghandi M, et al. Quantitative Proteomics of the Cancer Cell Line Encyclopedia. *Cell*. 2020 Jan 23;180(2):387-402.e16.
- [12] Uhlén M, Fagerberg L, Hallström BM, et al. Tissue-based map of the human proteome. *Science*. 2015 Jan 23;347(6220):1260419.
- [13] Liu CJ, Hu FF, Xia MX, et al. GSCALite: a web server for gene set cancer analysis. *Bioinformatics*. 2018 Nov 1;34(21):3771-3772.
- [14] Szklarczyk D, Gable AL, Lyon D, et al. STRING v11: protein-protein association networks with increased coverage, supporting functional discovery in genome-wide experimental datasets. *Nucleic Acids Res*. 2019 Jan 8;47(D1):D607-D613.
- [15] Yang W, Soares J, Greninger P, et al. Genomics of Drug Sensitivity in Cancer (GDSC): a resource for therapeutic biomarker discovery in cancer cells. *Nucleic Acids Res*. 2013 Jan;41(Database issue):D955-61.

- [16] Rees MG, Seashore-Ludlow B, Cheah JH, et al. Correlating chemical sensitivity and basal gene expression reveals mechanism of action. *Nat Chem Biol.* 2016 Feb;12(2):109-16.
- [17] Li T, Fu J, Zeng Z, et al. TIMER2. 0 for analysis of tumor-infiltrating immune cells. *Nucleic Acids Res.* 2020 Jul 2;48(W1):W509-W514.
- [18] Mermel CH, Schumacher SE, Hill B, et al. GISTIC2. 0 facilitates sensitive and confident localization of the targets of focal somatic copy-number alteration in human cancers. *Genome Biol.* 2011;12(4):R41.
- [19] Fu J, Li K, Zhang W, et al. Large-scale public data reuse to model immunotherapy response and resistance. *Genome Med.* 2020 Feb 26;12(1):21.
- [20] Apetoh L, Ghiringhelli F, Tesniere A, et al. Toll-like receptor 4-dependent contribution of the immune system to anticancer chemotherapy and radiotherapy. *Nat Med.* 2007 Sep;13(9):1050-9.
- [21] Mariathasan S, Turley SJ, Nickles D, et al. TGF- β attenuates tumour response to PD-L1 blockade by contributing to exclusion of T cells. *Nature.* 2018 Feb 22;554(7693):544-548.
- [22] Deguchi A, Maru Y. Inflammation-associated premetastatic niche formation. *Inflamm Regen.* 2022 Jul 3;42(1):22.
- [23] Yao D, Dong M, Dai C, et al. Inflammation and Inflammatory Cytokine Contribute to the Initiation and Development of Ulcerative Colitis and Its Associated Cancer. *Inflamm Bowel Dis.* 2019 Sep 18;25(10):1595-1602.
- [24] Seki E, De Minicis S, Österreicher CH, et al. TLR4 enhances TGF- β signaling and hepatic fibrosis. *Nat Med.* 2007;13:1324–32.
- [25] Bhowmick NA. TGF- β signaling in fibroblasts modulates the oncogenic potential of adjacent epithelia. *Science.* 2004;303:848–51.
- [26] Deguchi A, Tomita T, Ohto U, et al. Eritoran inhibits S100A8-mediated TLR4/MD-2 activation and tumor growth by changing the immune microenvironment. *Oncogene.* 2016;35:1445–56.
- [27] Wu Z, Mehrabi Nasab E, Arora P, et al. Study effect of probiotics and prebiotics on treatment of OVA-LPS-induced of allergic asthma inflammation and pneumonia by regulating the TLR4/NF-kB signaling pathway. *J Transl Med.* 2022 Mar 16;20(1):130.

- [28] Luo L, Wall AA, Yeo JC, et al. Rab8a interacts directly with PI3K γ to modulate TLR4-driven PI3K and mTOR signaling. *Nat Commun.* 2014 Jul 15;5:4407.
- [29] Fan W, Morinaga H, Kim JJ, et al. FoxO1 regulates Tlr4 inflammatory pathway signaling in macrophages. *EMBO J.* 2010 Dec 15;29(24):4223-36.
- [30] Murshid A, Borges TJ, Lang BJ, et al. The Scavenger Receptor SREC-I Cooperates with Toll-Like Receptors to Trigger Inflammatory Innate Immune Responses. *Front Immunol.* 2016 Jun 13;7:226.
- [31] Hu J, Xu J, Feng X, et al. Differential Expression of the TLR4 Gene in Pan-Cancer and Its Related Mechanism. *Front Cell Dev Biol.* 2021 Sep 23;9:700661.
- [32] Sun M, Gu P, Yang Y, et al. Mesoporous silica nanoparticles inflame tumors to overcome anti-PD-1 resistance through TLR4-NF κ B axis. *J Immunother Cancer.* 2021 Jun;9(6):e002508.
- [33] Tsukamoto H, Kubota K, Shichiku A, et al. An agonistic anti-Toll-like receptor 4 monoclonal antibody as an effective adjuvant for cancer immunotherapy. *Immunology.* 2019 Oct;158(2):136-149.
- [34] Guo X, Du L, Ma N, Zhang P, Wang Y, Han Y, Huang X, Zhang Q, Tan X, Lei X, Qu B. Monophosphoryl lipid A ameliorates radiation-induced lung injury by promoting the polarization of macrophages to the M1 phenotype. *J Transl Med.* 2022 Dec 14;20(1):597.